ever, which population of bone marrow cells enter the brain and become neurons and what factor is involved in this process still need to be exactly deciphered. To this end, we used single cell-derived immortalized BMS cell lines in this study to determine which marrow cells differentiate into neural cells since separation of mesenchymal cells by commonly used methods such as Percoll gradient cannot eliminate the possibilities of contamination with hematopoietic cells. We therefore investigated cell lines which exhibited the morphological character of neural lineages through the action of a demethylating agent capable of altering gene expression (Holliday, 1996) as well as neural inducer Noggin on the basis that cardiomyocytes are generated from marrow stromal cells by 5-azacytidine (Makino et al., 1999).

Noggin is a diffusible factor involved in the neural induction during early embryogenesis (Smith and Harland, 1992) as well as adult neurogenesis (Lim et al., 2000) by antagonizing bone morphogenetic protein (BMP) signaling (Zimmerman et al., 1996). Furthermore, Noggin converts embryonic stem cells into primitive neural stem cells by the inhibition of BMP-related signaling (Tropepe et al., 2001). On the basis of these findings, we hypothesized that Noggin might antagonize BMP signaling which is necessary for osteogenesis of BMS cells and thus induce the differentiation of BMS cells into neural lineages. Neurons derived from BMS cells were examined for neuron-specific cell markers and gene expression, and were characterized electrophysiologically. Neurons could be generated from a specific fraction of BMS cells that we have been able to characterize.

Methods

Cell culture and transplantation

Dexter long-term bone marrow cultures derived from the bone marrow of female C3H/He mice were established as described (Whitlock and Witte, 1982, 1987; Umezawa et al., 1991, 1992). Cell lines from different dishes were subcloned by limiting dilution, and clones were designated NRG (*neurogenic*), KUM9 and KUSA/A1. The differentiation protocols to induce adipogenesis, osteogenesis, and myogenesis were followed as described (Pittenger et al., 1999, 2000).

To determine *in vivo* osteogenic activity, KUSA/A1 cells were transplanted subcutaneously. Six weeks after the transplantation, the tumor was excised for analysis.

Measurement of alkaline phosphatase (ALP) activity

BMS cells were analyzed by ALP assay as described (Leboy et al., 1991). The ALP activity was measured with an ALP B-test Waco kit (Waco) based on the method of Lowry-Bessey (Bessey et al., 1946). Fifty microliters of homogenate was incubated with the assay buffer at 37°C, and the reaction was spectrophotometrically measured at 405 nm.

5-azacytidine protocol for neuronal differentiation

Cells were cultured in IMDM supplemented with 10% FBS and streptomycin/penicillin at 33°C in humid air with 5% CO2. For induction of cell differentiation, cells were treated with 10 umol/l of 5-azacytidine (Sigma Chemical Co) for 96 h in IMDM medium supplemented 10% FBS containing 50 ng/ml of nerve growth factor (NGF), brain-derived neurotrophic factor (BDNF) and neurotrophin-3 (NT-3) on a 60 mm dish that had been coated with poly-L-ornithine (Sigma) and fibronectin (Gibco BRL) (ornithine/fibronectin). After the induction protocol, medium was replaced with B27-supplemented DMEM/F12 (DMEM/F12/B27, Gibco BRL) containing 50 ng/ml of NGF, NT-3 and BDNF (NGF/NT3/BDNF).

xNoggin protocol for neuronal induction

KUSA/A1 cells were cultured in IMDM supplemented with 10% FBS and streptomycin/penicillin at 33°C in humid air with 5% CO2. KUSA/A1 cells were transfected with xNoggin/MC BOS (a gift of Dr Yoshiko Takahashi) (Tonegawa and Takahashi, 1998) and neo (10:1) by liposomal transfection using Fugene. G418 were added into the medium 24 h after transfection. Seven to ten days after transfection, cell aggregates were detached from the dish and formed neurosphere-like cluster. Cluster-forming cells were dissociated by triturating using a Pasteur pipette, resuspended in DMEM/F12/B27 supplemented with 5% FBS containing 20 ng/ml bFGF, and then passaged on a 60 mm dish coated with ornithine/fibronectin. Medium was replaced with DMEM/F12/B27 containing 50 ng/ml NGF/NT-3/BDNF four days after the passage.

Reverse transcription and polymerase chain reaction (RT-PCR)

Total RNA was extracted from NRG, KUM9 and KUSA/A1 cells (on Day 0, 2, 4, and 9) and adult mouse cerebrum by ISOGEN (Nippon gene). RT-PCR of neuron-specific genes, including NCAM, growth-associated protein-43 (GAP-43), Trk A, Trk B, Trk C and G3PDH was performed using 3 μg of total RNA. PCR was performed for 30–35 cycles, with each cycle consisting of 95°C for 30 s, 53–60°C for 1.5 min, and 72°C for 1 min, with an additional 7-min incubation at 72°C after completion of the last cycle. The primers used were follows: NCAM, CTCCCTGCCTCCAACCATCATC and TCTCGTCATCTTCCTCCTCGTTCTC; GAP43, GATGGCTCTGCTACTACC and TCGGCTTGTTTAGGCTCC; Trk A, CTGGGCGGAGTGCCTGAA and GGCTGCCGGCTCCAGGAA; Trk B, AATGAAACAAGCCACACACAGGGC and TGGAGTGTTACTCCCATTGGAGAT; TrkC, AATTGAGGAGGAGCGGGGAC and GACATGCCCAGAGGATAGCG; G3PDH, GACCACAGTCCATGCCATCACT and TCCACCACCCTGTTGCTGTAG.

Immunocytochemistry

After cells were washed twice with PBS, the cells were fixed with 4% paraformaldehyde for 15 min. After incubation with 10% normal goat serum, the cells were reacted with anti-MAP2 antibody (Sigma), anti-TujI antibody (Sigma), anti-NeuN antibody (Chemicon international, Inc.), anti-Hu antibody (Marusich et al., 1994), anti-GFAP antibody (DAKO), and anti-Gal-C antibody (Sigma) in PBS containing 1% bovine serum albumin. As a methodological control, the primary antibody was omitted. After washing in PBS, slides were incubated with Peroxidase-conjugated anti-mouse immunoglobulin antibody or anti-rabbit immunoglobulin antibody (EnVision, DAKO, co., K4001, CA). Cells were stained using a solution containing 3, 3'-diaminobenzidine (DAB), 10 mM sodium azide, and 0.01% H_2O_2 in 0.05 M Tris-HCl buffer, pH 6.7.

Patch clamp recording procedure

A coverslip to which cultured cells had adhered was placed in a recording chamber, and the chamber was mounted on the stage of an inverted microscope equipped with Nomarski optics (IX-70, Olympus, Japan) and a ×60 objective lens. The chamber was continuously perfused with solutions gravity-fed at a rate of approximately 1 ml/min at room temperature (approximately 25°C). Membrane voltages and currents were recorded by a patch clamp method in the whole-cell configuration. The patch pipette was made of Pyrex tubing pulled on a micropipette puller (P-87, Sutter Instrument, Novato, CA). The recording pipette was connected to the input stage of a patch clamp amplifier (Axopatch 200B, Axon Instruments, Foster City, CA). An Ag-AgCl wire connected to the bath via a ceramic bridge served as an indifferent electrode. The pipette resistance was approximately 10 MΩ when filled with pipette solution. The input capacitance and the series resistance electrically compensated as much as possible. Recorded signals were low-pass filtered (Bessel filter, cut-off frequency 5 kHz) and sampled at 10 kHz with a DigiData 1200 interface and pCLAMP 8 software (Axon Instruments).

To analyze the patch clamp recording, cells were transfected with P/Tα1:EYFP plasmid by the lipofection method using Fugene™ 6 (Roche Diagnostic Corporation). Outwardly rectifying K^+ currents were recorded by voltage-clamping the cell membrane to −97 mV, stepping to test voltages between −107 mV and +63 mV in 10 mV increments for 100 msec and returning to the initial holding potential.

Calcium imaging

Calcium imaging was performed by confocal microscopy of cultured cells loaded with fluo-3 acetoxymethylester (2 μM; Molecular Probes, Eugene, Oregon). A BioRad MRC600 confocal scanning microscope, equipped with a krypton/argon laser (488 nm line), was used to obtain images of the fluo-3 signal. The emission fluorescence was measured through a 520 to 560 nm interference filter. The cells were challenged with a depolarizing stimulus of 135 mM potassium, 100 mM glutamate and 100 mM acetylcholine by bath applications. Image analysis was performed using Igor Pro software (WaveMetrics, Lake Oswego, OR) with custom-made procedures. Areas were normalized to the control response with the standard external solution and shown with colored scale. The standard external solution for patch clamp and Ca^{2+} imaging experiments contained (in mM) NaCl 135, KCl 2.5, $CaCl_2$ 2, $MgCl_2$ 1, HEPES 10 and glucose 10 (pH 7.4), and the standard pipette solution for patch clamp experiments contained (in mM) NaCl 10, K gluconate 130, $CaCl_2$ 1, EGTA 1.1, HEPES 10 and ATP-Na_2 2 (pH 7.2).

Fluorescence activated cell analysis

All samples were treated by water lysis. Cells, at a final concentration of 1×10^7/ml, were incubated with 1 mg of a monoclonal antibody in Hank's balanced salt solution (containing 0.1% of albumin and 0.1% of sodium azide). In case that the first antibody is conjugated with biotin, cells were then washed twice and incubated with 1 mg of streptoavidin-phycoerythrin (Gibco BRL) for 30 minutes on ice. Purified antibodies in the first step were stained with 1 mg of FITC-conjugated goat anti-mouse antibody. Controls included cells stained with individual isotype (mouse IgG1 or rat IgG2a). Incubations were performed in the presence of 10 mg of mouse immunoglobulin to prevent nonspecific antibody binding. Antibodies (anti-mouse Flk-1, CD31, CD34, c-kit, Sca-1, CD140a, CD144, CD14, CD29, CD41, CD44, CD49b, CD49d, CD54, CD90, CD102, CD106, Ly-6C, and Ly-6G, and isotype control antibodies) were purchased from Pharmingen Pharmaceutical, Inc. (San Diego, CA). After 2 washes with Hank's balanced salt solution, in order to remove dead cells, propidium iodide (PI) was added to each test tube at a concentration of 1 mg/ml just before acquisition by FACScan flow cytometry (Beckton Dickinson) with the Argon laser at 488 nm. List mode data for 30,000 to 50,000 cells were collected in PI gate.

Results

To know the pluripotency and plasticity of BMS cells, we investigated neurogenesis in marrow-derived BMS cells. We isolated several clones from adult female C3H/He mice by frequent subculture. The clones could differentiate into osteogenic, adipogenic, and myogenic lineages in specific culture conditions (Fig. 1). The BMS cells showed a fibroblastic appearance without any treatment. We employed KUM9, NRG, and KUSA/A1 with several differentiation protocols (Pittenger et al., 1999) (Fig. 1). KUM9 cells exhibited several mesenchymal phenotypes including osteocytes, adipocytes, and myocytes, and NRG cells could differentiate into osteocytes and adipocytes. Interestingly, KUSA/A1 could only be otherwise induced to form osteoblasts and exhibit osteogenesis *in vivo* (Fig. 1a and b). KUSA/A1, NRG, and KUM9 exhibited extremely high alkali phosphatase activity, indicating that these cells have an osteogenic potential (Fig. 1c). We did not obtain cardiomyocytes from these clones.

We then characterized them with surface markers (Fig. 1d and e). Both KUM9 and NRG cells were positive for CD34 (hematopoietic stem cell markers), Sca-1 (Ly-6A/E), CD140 (platelet derived growth factor receptor-α), CD29 (Integrin 1), CD44 (Pgp-1/Ly-24), and Ly-6C; and negative for Flk-1 (KDR or VEGF-receptor2), CD31 (PECAM-1), c-kit (CD117), CD14 (a marker for macrophages and dendritic cells, and lipopolysaccharide receptor), CD144 (vascular endothelium cadherin or cadherin5), CD14, CD45 (leukocyte common antigen), CD49b (integrin α2), CD49d (integrin α 4), CD54 (ICAM-1), CD90 (Thy-1), CD102 (ICAM-2), CD105 (endoglin or TGF-β receptor), and CD41 (integrin α IIb or platelet glycoprotein IIb). CD106 (VCAM-1) was detected in KUM9 cells, but not NRG cells. Surface marker analysis indicated that the cells exhibited markers for osteoblasts such as CD44 and Ly-6C; myeloid cells, Sca-1; and mesenchymal cells, CD140, indicating that these cells are of mesenchymal origin as well as morphological features. These cells did not express CD105, TGF-β receptor, while mesenchymal stem cells are reported to be positive for CD105 (Pittenger et al., 1999).

Neural differentiation was induced by 5-azaC, a demethylating agent (Fig. 2a). The BMS cells showed a fibroblastic appearance before treatment, and the morphology of the cells changed gradually, but dramatically on Day 4 (Fig. 2b). Approximately 20% of NRG and KUM9 cells formed neurite-like processes and showed a neuron-like morphology on Day 9. Immunocytochemistry revealed that the cells were positive for neuron-speci-

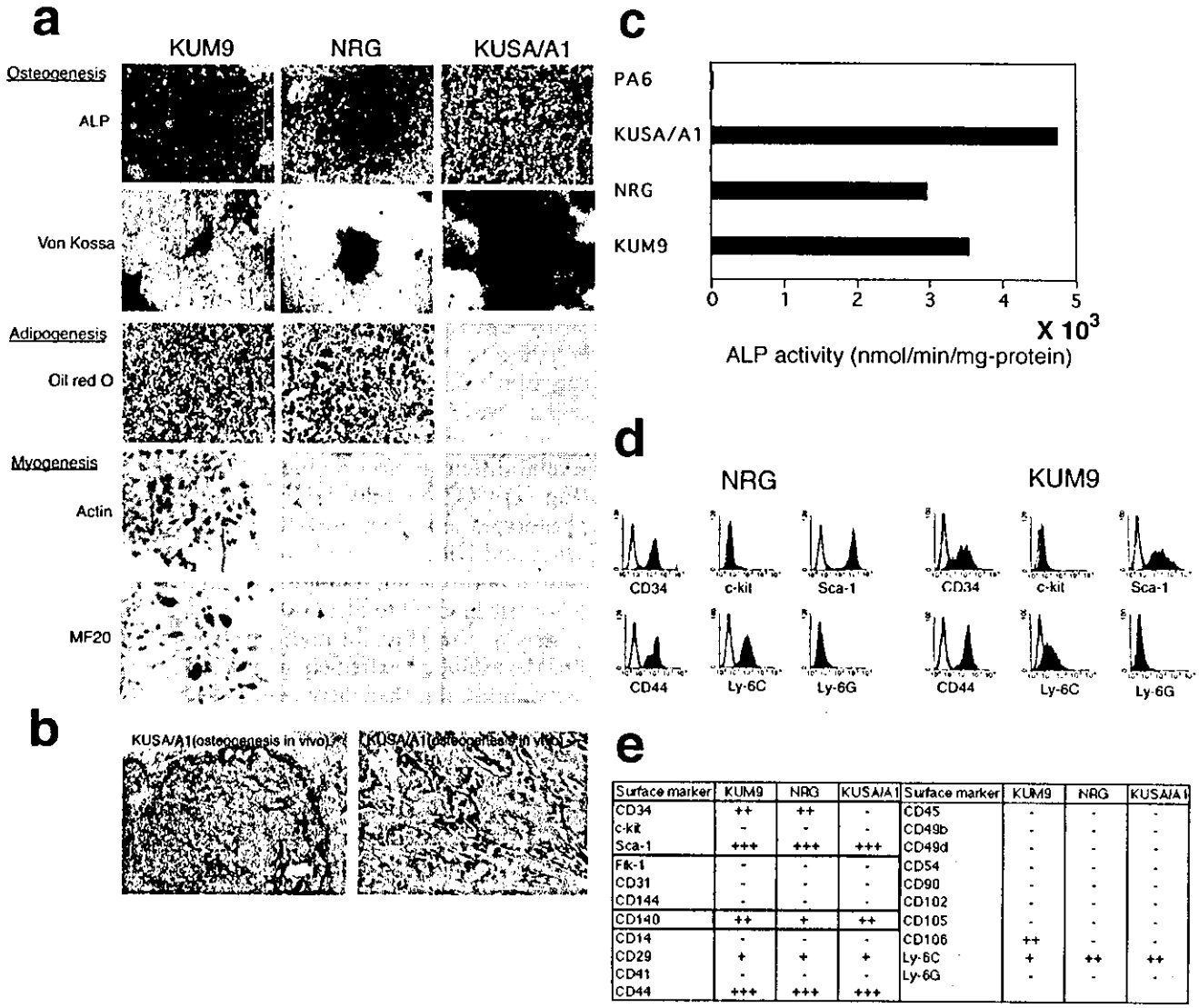

Surface marker	KUM9	NRG	KUSA/A1	Surface marker	KUM9	NRG	KUSA/A1
CD34	++	++	-	CD45	-	-	-
c-kit	-	-	-	CD49b	-	-	-
Sca-1	+++	+++	+++	CD49d	-	-	-
Flk-1	-	-	-	CD54	-	-	-
CD31	-	-	-	CD90	-	-	-
CD144	-	-	-	CD102	-	-	-
CD140	++	+	++	CD105	-	-	-
CD14	-	-	-	CD106	++	-	-
CD29	+	+	+	Ly-6C	+	++	++
CD41	-	-	-	Ly-6G	-	-	-
CD44	+++	+++	+++				

Fig. 1 Multiple differentiated phenotypes of isolated BMS cells which have a neurogenic potential. **(a)** The stromal KUM9, NRG and KUSA/A1 cells exposed to conditions that normally induce adipogenesis, osteogenesis, and myogenesis. Osteogenic, adipogenic, and myogenic differentiation were separately induced in the stromal clones. Adipogenic differentiation was observed in NRG and KUM9 cells with accumulation of lipid vacuoles within cells and staining of the vacuoles with Oil red O. Osteogenic differentiation was confirmed by alkaline phosphatase activity in all the cells tested. KUSA/A1 cells exhibited extremely high alkaline phosphatase activity, and aggregated and formed nodules. KUM9 cells could give rise to myocytes which was positively stained with anti-MF20 and anti-actin antibodies. **(b)** *In vivo* osteogenic activity by KUSA/A1 cells. (*right*) High-power view of bone trabeculae generated by KUSA/A1. H.E. stain. **(c)** Quantitative analysis of alkali phosphatase activity was performed on each cell after MC3T3-PA6 preadipocytes (Kawasaki et al., 2000), KUSA/A1, NRG and KUM9 cells exposed to conditions that induce osteogenesis. **(d)** Representative results of flow cytometric analysis in NRG and KUM9 cells. NRG (*left*) and KUM9 (*right*) cells were stained with FITC-conjugated antibodies. Flow cytometric curve with these antibodies is shown in gray with the isotype control curve. **(e)** Further phenotypic analysis in KUM9, NRG and KUSA/A1.

fic markers including TujI, Hu, and NeuN, suggesting that they could be induced into neurons (Fig. 3a-e and g). To determine whether BMS cells may also be induced to differentiate into astrocytes or oligodendrocytes, NRG, KUM9, and KUSA/A1 cells were immunohistochemically stained by glial markers (Fig. 3f, h, i, and l). These cells were positive for GFAP and Gal-C. Furthermore, the differentiated NRG, KUM9 and KUSA/A1 cells expressed neuron-specific genes such as Trk A, Trk B, Trk C, NCAM, and GAP-43 (Fig. 3o). Interestingly, the number of the positive cells differed among the cell lines (Fig. 3p), indicating that each cell line contained several committed progenitors that independently give rise to neurons, astrocytes and oligodendrocytes. These results suggest that these cells could be transformed into neurons, astrocytes, and oligodendrocytes.

We next attempted to devise a system for regeneration of functional neurons without 5-azaC treatment. Based on the evidence that (i) Noggin is an inducer of neural cell lineage in *Xenopus* development (Lamb et al., 1993), (ii) Noggin creates a niche for adult neurogenesis in mammals (Lim et al., 2000), (iii) Noggin is a BMP2/4 antagonist and thus may inhibit osteogenic activities of the cells (Zimmerman et al., 1996), we examined whether Noggin could induce BMS cells to form neurons (Fig. 4). Four days after transfection, KUSA/A1 cells began to aggregate and detach from the dishes. The detached cells formed floating neurosphere-like clusters. When cluster-forming KUSA/A1 cells were transferred onto ornithine/fibronectin-precoated dishes, almost all the cells exhibited a mature neuron-like morphology, including characteristic axons, axon terminals, and a refractile round cell body (Fig. 4a–e), and more than 50% of the cells became immunocytochemically positive for MAP2 (Fig. 4f). Interestingly, this Noggin-based protocol reduced the proportion of astrocytes to ~5% and increased that of neurons (Fig. 4g). Since BMP2 inhibits neurogenesis and concomitantly promotes astrogenesis of neural stem cells (Nakashima et al., 1999; Nakashima et al., 2001), antagonistic activity of Noggin to BMP2 may suppress astrocytic differentiation increasing the efficiency of neuron formation.

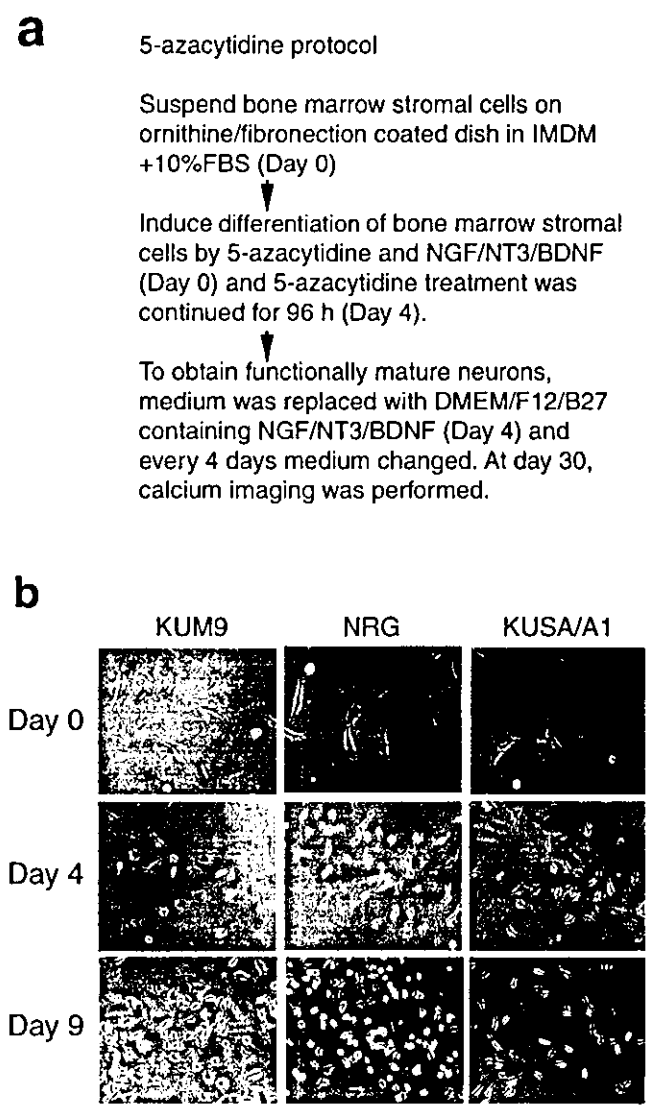

Fig. 2 A simple protocol for induction of "meta-differentiation" of BMS cells to neurons. (a) 5-azacytidine (5-azaC) protocol. Neurons could be generated from KUM2 subline (NRG), KUM9 and KUSA/A1 cells *in vitro*. (b) The cells showed fibroblast-like morphology before 5-azaC treatment and its morphology changed dramatically by Day 4. Approximately 20% of the NRG, KUM9 and KUSA/A1 cells formed neurite-like processes on Day 9.

We then characterized the electrophysiological properties of neurons from BMS cells. To visualize neuronal cells alive among mixed cell population, NRG cells were transfected with P/Tα1:EYFP (Sawamoto et al., 2001) and exposed to 5-azaC (Fig. 5a), since the marker fluorescence driven by the α1-tubulin promoter is selectively expressed in precursors and young neurons (Roy et al., 2000; Sawamoto et al., 2001). Electrophysiological properties of these identified neuronal cells were analyzed by whole-cell patch clamp recording. 5-azaC treatment led to a decrease in resting membrane potential to −20 mV on Day 14, and −50 mV on Day 28 by whole-cell patch clamp recording. Such a resting membrane potential was also observed in neurons which served a positive control. Furthermore, we have measured ionic currents by the patch clamp method under voltage clamp condition (Fig 5b). With the increase of the voltage, rectifying current was clearly detected, indicating the presence of voltage-dependent K^+ current. These results suggest that K^+ channels started to be expressed concomitantly with the morphological change and the increased expression of the neuron-specific markers. The induction of potassium channel in differentiating BMS cells seems to be in accordance with the evidence that the expression of potassium channel parallels the maturation of cell excitability and neural differentiation throughout development (Ribera and Spitzer 1992; Ribera, 1999).

To determine the ability of neurons derived from BMS cells to respond to depolarizing stimuli, we loaded NRG cells with the calcium indicator dye fluo-3 and exposed them to high potassium (Fig. 5c). NRG cells treated with 5-azaC showed a rapid and reversible calcium increase in response to acetylcholine, a response characteristic of functional neurons (Pincus et al., 1998; Roy et al., 2000). Calcium increase was also determined in neurons obtained using the Noggin protocol in response to neurotransmitters and elevated potassium on Day 28. KUSA/A1-derived neurons clearly responded to potassium and glutamate (Fig. 5d–i). The calcium uptake was observed immediately after the stimulation of high potassium (Fig. 5g), which is probably resulted from opening of Ca^{2+} channel by depolarization with high potassium. These results suggest that functional mature neurons could be generated from BMS cells ex-

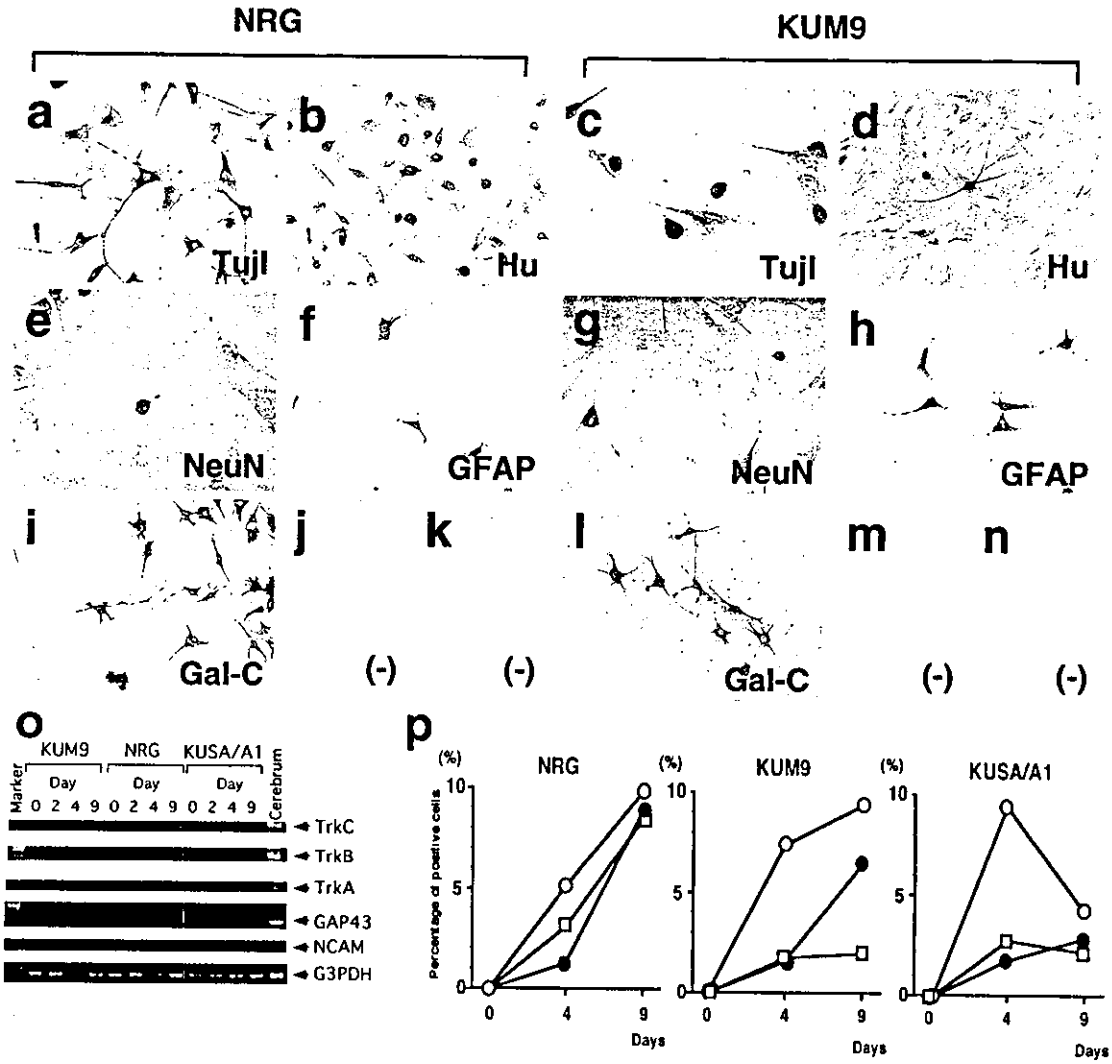

Fig. 3 Neurogenic differentiation of BMS cells with 5-azaC treatment (**a–n**) Immunohistochemical analysis of the stromal cell-derived neural cells. NRG and KUM9 cells were stained with anti-tubulin (TujI, **a** and **c**), anti-Hu (**b**, **d**), anti-NeuN (**e**, **g**), anti-GFAP (**f**, **h**), and anti-Gal-C (**i**, **l**) antibodies. As negative controls, these cells were stained with anti-mouse immunoglobulin antibody (**j**, **m**) or anti-rabbit immunoglobulin antibody (**k**, **n**). (**o**) RT-PCR was used to determine expression of the neuron-specific genes including trkA, trkB, trkC, GAP-43, and N-CAM. C3H/He mouse cerebrum was used as a positive control. The cells did not express any genes on Days 0 and 2. Expression of trkA was observed in NRG and KUSA/A1 cells on Day 9. trkB was expressed in KUM9, NRG and KUSA/A1 on Day 9. trkC was expressed in KUM9 cells on Days 4 and 9, and in NRG and KUSA/A1 cells on Day 9. GAP-43 was expressed in all the tested cell on Days 4 and 9. NCAM was expressed in KUM9 cells on Days 4 and 9, and in NRG and KUSA/A1 cells on Day 9. (**p**) Time-kinetics of expression of TujI, GFAP and Gal-C proteins was determined by immunohistochemistry. The BMS cells were treated with 5-azaC, fixed on Days 0, 4 and 9, and then stained with anti-TujI (*open circle*), anti-GFAP (*open square*) and anti-Gal-C (*closed circle*) antibodies, and the number of immunoreactive cells per field at 200 ± configuration was counted and given as a percentage of total cells.

posed to Noggin. Immunocytochemistry confirmed that these cells were positive for TujI.

Discussion

We have devised an efficient and simple system for controlled regeneration of neurons from marrow stroma-derived bone cells. Particular fractions of oligo-potent KUM9 or bipotent NRG were found to start expressing neuronal markers with exposure to a demethylating agent. Moreover, one hundred percent of KUSA/A1 express markers for osteoblasts at a high level, as determined by enzyme histochemistry and flow cytometric analysis. We thus conclude that isolated mature osteoblasts can be converted into functional neurons using the single cell-derived clonal KUSA/A1. Extensive characterization of this unique cell line enabled us to define this potential source of neurons. In contrast, MC3T3/PA6 stromal cells, which have an adipogenic potential

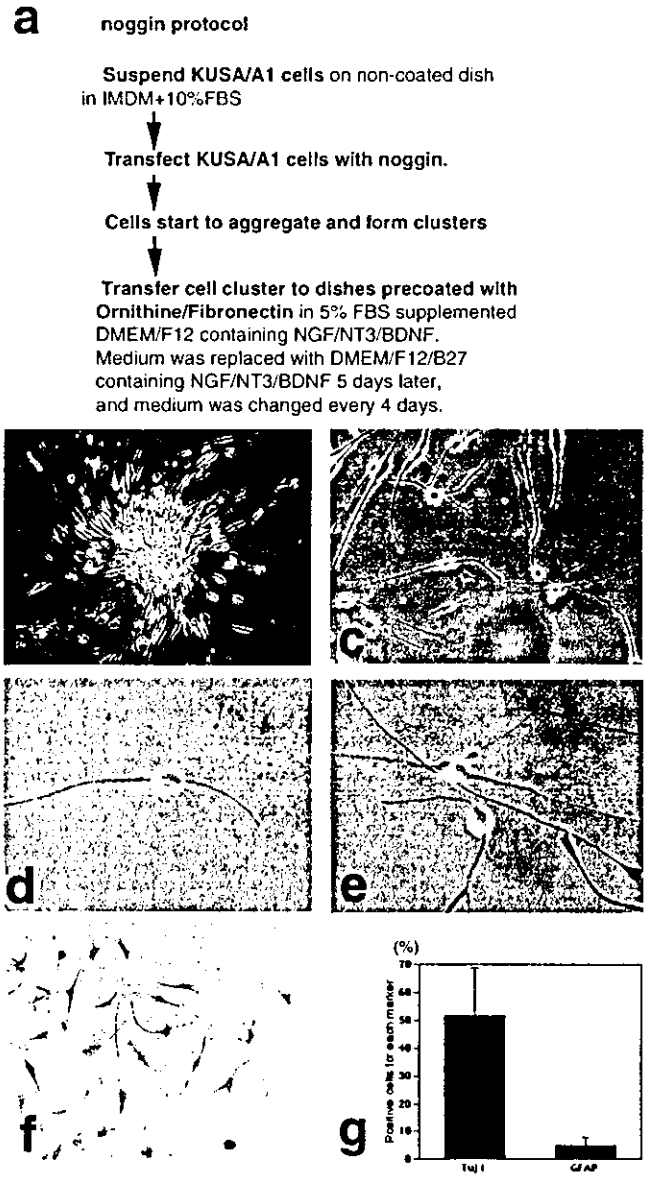

Fig. 4 Efficient Noggin protocol for neuronal induction. (a) Noggin protocol. (b–e) The cells had a round cell body, neurite-like spikes (>80%) and terminated forming an axon terminal-like appearance. (f) Immunohistochemical analysis of KUSA/A1 cells with the Noggin protocol. Immunocytochemical analysis with anti-MAP2 antibody was performed 2 weeks after the transfer of cell clusters to the ornithine/fibronectin coated dish. (g) Percentage of cells positive for MAP2 were counted. The proportion of the cells positive for GFAP, an astrocytic marker, with the Noggin protocol decreased in comparison to 5-azaC-based protocol.

and were recently reported to induce neurogenic differentiation of ES cells (Kawasaki et al., 2000), did not differentiate into neurons (data not shown). Our results reveal that mesoderm-derived BMS cells with osteogenic activity have a surprising plasticity to an ectodermal endpoint. We have also shown that neurons converted from osteoblasts respond to physiological transmitters just like neurons generated from human adult neural stem cells (Roy et al., 2000).

BMS cells include multipotent progenitors which are able to differentiate into adipogenic, chondrogenic, myogenic, osteogenic, and cardiomyogenic lineages. However, differentiated phenotypes are limited to mesoderm-derived tissues. Demethylating agents have been used to induce cell differentiation into multiple lineages via modifying methylation/chromatin status which is precisely regulated during development (Umezawa et al., 1997). Here, the question is the mechanism underlying the conversion of a cell of mesodermal origin into that of ectodermal origin. 5-azaC is a cytidine analog with a nitrogen atom replacing the carbon at the 5 position of the pyrimidine ring. 5-azaC treatment results in hypomethylation of genes due to blocking methylation in replicating cells and/or inhibiting of methyltransferase, leading to gene expression (Holliday et al., 1996). The possible mechanisms of 5-azaC effect are (i) reversion of differentiated BMS cells to an immature pluripotent state in which they could differentiate into ectodermal, endodermal, and mesodermal lineages, (ii) induction of differentiation of pluripotent BMS cells present among the population, and (iii) transdifferentiation of mesodermal derivatives into ectodermal ones. 5-azaC is also reported to be a potent agent for maturation of neurons generated from neural stem cells (Schinstine and Iacovitti, 1997) indicating BMS cells may have a potential of neural stem cells and 5-azaC acts as a maturation inducing factor for neurogenesis.

We also adopted Noggin, a BMP2/4 antagonist (Zimmerman et al., 1996), as an inducible factor for generation of neurons, since Noggin participates in neurogenesis in *Xenopus* development (Lamb et al., 1993), and creates a niche for adult neurogenesis in mammals (Lim et al., 2000). Noggin-treated mature osteoblasts converted into neurons efficiently, suggesting that Noggin likewise has a pivotal role on transdifferentiation from BMS cells to neurons. Compared to 5-azaC treatment, Noggin suppressed generation of astrocytes from KUSA/A1 cells. Since BMPs induce astrocytic differentiation and inhibit neurogenesis (Nakashima et al., 2001), it is conceivable that the effect of Noggin as a BMP2/4 antagonist suppressed astrocytic differentiation and increased the proportion of neuronal formation (Lim et al., 2000). Moreover, the effect of Noggin as a BMP2/4 antagonist may play a critical role for neurogenesis from osteoblasts, since KUSA/A1 highly expressed BMPs (Ko, MSH, unpublished observation). Because BMPs induce the differentiation of mesenchymal cells into osteogenic cells (Wang et al., 1990; Hughes et al., 1995), antagonists of BMPs may inhibit osteocytic differentiation of KUSA/A1 and thus accelerate differentiation into a neural lineage. The Noggin protocol that cells were converted to a different germ layer with specific inducers, sphere formation, coating, and maturation is quite interesting since the protocol did not in-

clude treatment of methylation/chromatin modifiers such as 5-azaC, sodium butyrate, and trichostatin.

The lineage interconversion between distinct adult committed precursors that originate from the same germ layer is rather surprising. There is limited *in vitro* evidence that adult stem cells exhibited differentiated phenotypes that were observed in different germ cell layers. Following *in vivo* transplantation, cells from the bone marrow can give rise to liver oval cells which are of endodermal origin (Petersen et al., 1999) as well as neuronal cells which are of ectodermal origin (Mezey et al., 2000). Expression of neurogenic phenotypes are observed in bone-originated sarcomas (Sugimoto et al., 1997). Lineage conversion between cells derived from different germ layers may occur in the levels of stem cells or multipotent precursors.

Stem cell biologists dream of the therapeutic use of stem cells for the recovery of damaged or degenerated

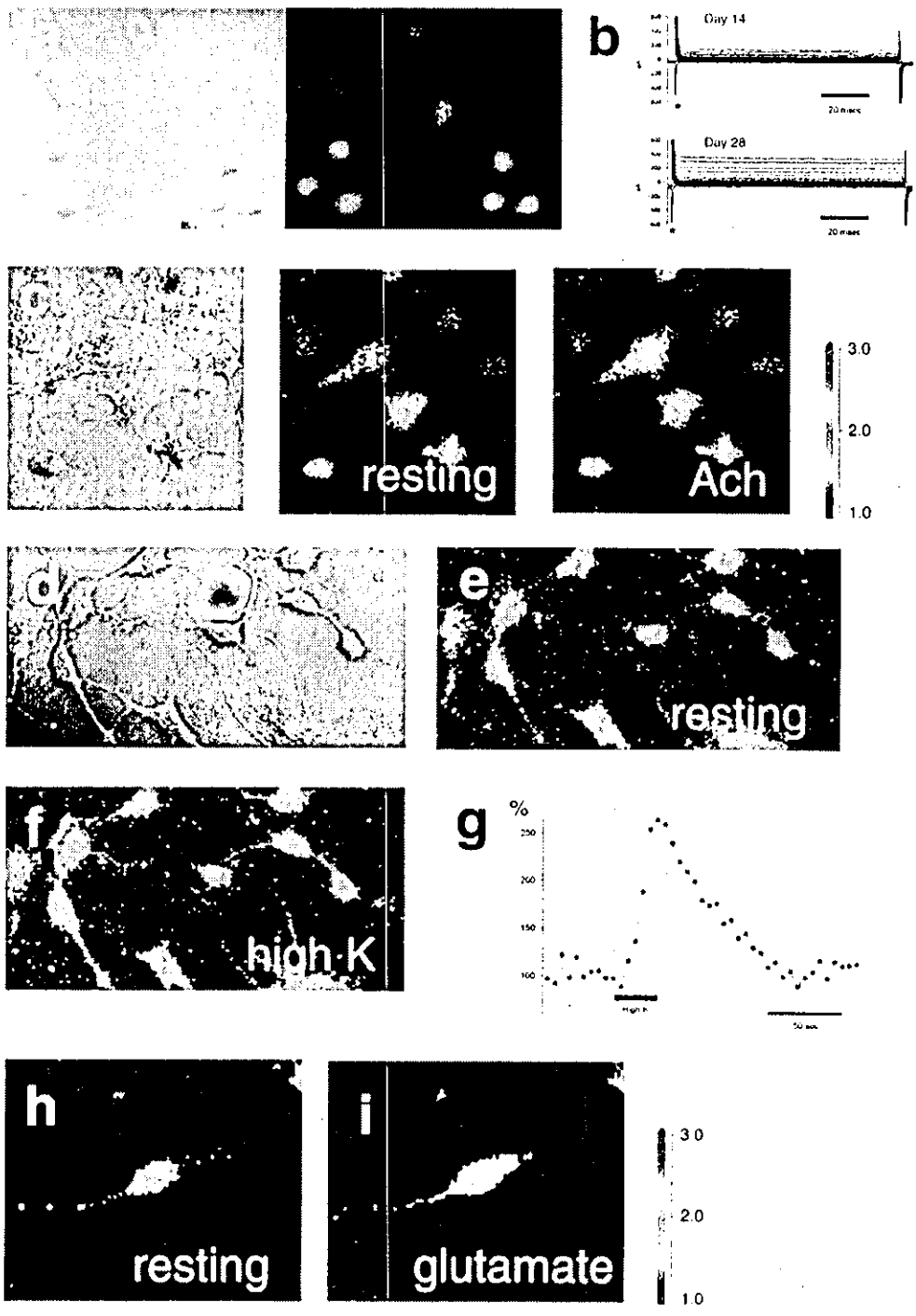

Fig. 5 Functional analysis of stromal cell-derived neurons. The function of stromal cell-derived neurons was evaluated by calcium imaging. **(a)** To identify functional mature neuron, PfTα1: EYFP-transfected NRG cells were treated with 5-azaC and maintained for 3–4 weeks (*left*: phase-contrast photomicrograph; *right*: fluorescent micrograph). **(b)** The electrophysiological properties were analysed on NRG cells on Day 14 (*upper column*) and Day 28 (*lower column*) after 5-azaC treatment. Artifacts immediately after the voltage command are shown by *asterisks*. **(c)** Calcium imaging of the 5-azaC-treated NRG cells before (*middle*) and after acetylcholine (labeled as *Ach*) treatment (*right*). Phase contrast micrograph is shown on the *left*. The cells showed rapid and reversible calcium uptake (250%) in response to acetylcholine. **(d–i)** The KUSA/A1 stromal cells with the Noggin protocol (details in Fig. 4) were also loaded with fluo-3 and were exposed to stimuli. The cells showed rapid and irreversible increases (364%) in cytosolic calcium in response to potassium **(d–g)**, and also responded to glutamate in a neuronal manner **(h, i)**. **(g)** Corresponding fluo-3 traces reveal that high potassium stimulation elevates calcium uptake in the KUSA/A1 with the Noggin protocol (*red*). The undifferentiated cells did not exhibit any response to high potassium in the same coverslip (*blue*).

organs. Marrow cells are routinely aspirated from patients and are therefore one of the most clinically practical sources of stem cells in adults. BMS cells are easy to culture and grow so rapidly. Therefore, these autologous cells have few practical, ethical, or immunological barriers to their clinical application and are a promising basis for future novel therapies.

Acknowledgements We are grateful to Dr. Yoshiko Takahashi for xNoggin/MC BOS. We also thank A. Thomson for critically reviewing the manuscript, K. Sakurada, F. Konishi, S. Higashi, Y. Uchida, T. Takizawa, W. Ochiai, M. Yanagisawa, Y. Takahashi, Y. Izawa, M. Fukuma, J. Ozawa, M. Takamatsu, S. Kusakari, Y. Yamada and T. Yamada for advice, and A. Kaneko for technical advice and discussion. This work was supported by a grant from the Ministry of Education, Science and Culture, and by Keio University Special Grant-in-Aid for Innovative Collaborative Research Project.

References

Ashton, B.A., Allen, T.D., Howlett, C.R., Eaglesom, C.C., Hattori, A. and Owen, M. (1980) Formation of bone and cartilage by marrow stromal cells in diffusion chambers in vivo. Clin Orthop 151:294–307.

Bessey, O.A., Lowry, O.H. and Breck, M.J. (1946) A method for the rapid determination of alkaline phosphatase with cubic millimeters of serum. J Cell Biol 164:321–326.

Bjornson, C.R., Rietze, R.L., Reynolds, B.A., Magli, M.C. and Vescovi, A.L. (1999) Turning brain into blood: a hematopoietic fate adopted by adult neural stem cells in vivo. Science 283:534–537.

Brazelton, T.R., Rossi, F.M., Keshet, G.I. and Blau, H.M. (2000) From marrow to brain: expression of neuronal phenotypes in adult mice. Science 290:1775–1779.

Clarke, D.L., Johansson, C.B., Wilbertz, J., Veress, B., Nilsson, E., Karlstrom, H., Lendahl, U. and Frisen, J. (2000) Generalized potential of adult neural stem cells. Science 288:1660–1663.

Dexter, T.M., Allen, T.D. and Lajtha, L.G. (1977) Conditions controlling the proliferation of haemopoietic stem cells in vitro. J Cell Physiol 91:335–344.

Ferrari, G., Cusella-De Angelis, G., Coletta, M., Paolucci, E., Stornaiuolo, A., Cossu, G. and Mavilio, F. (1998) Muscle regeneration by bone marrow-derived myogenic progenitors. Science 279:1528–1530.

Fuchs, E. and Segre, J.A. (2000) Stem cells: a new lease on life. Cell 100:143–155.

Harigaya, K., Cronkite, E.P., Miller, M.E. and Shadduck, R.K. (1981) Murine bone marrow cell line producing colony-stimulating factor. Proc Natl Acad Sci USA 78:6963–6966.

Holliday, R. (1996) DNA methylation in eukaryotes: 20 years on. In: In: Russo, V.E.A., Martienssen, R.A., Riggs, A.D. (eds) Epigenetic mechanisms of gene regulation Cold Spring, Harbor Laboratory Press, pp 5–27.

Hughes, F.J., Collyer, J., Stanfield, M. and Goodman, S.A. (1995) The effects of bone morphogenetic protein-2 -4 and -6 on differentiation of rat osteoblast cells in vitro. Endocrinology 136:2671–2677.

Kawasaki, H., Mizuseki, K., Nishikawa, S., Kaneko, S., Kuwana, Y., Nakanishi, S., Nishikawa, S.I. and Sasai, Y. (2000) Induction of midbrain dopaminergic neurons from ES cells by stromal cell-derived inducing activity. Neuron 28:31–40.

Lamb, T.M., Knecht, A.K., Smith, W.C., Stachel, S.E., Economides, A.N., Stahl, N., Yancopolous, G.D. and Harland, R.M. (1993) Neural induction by the secreted polypeptide noggin. Science 262:713–718.

Leboy, P.S., Beresford, J.N., Devlin, C. and Owen, M.E. (1991) Dexamethasone induction of osteoblast mRNAs in rat marrow stromal cell cultures. J Cell Physiol 146:370–378.

Lim, D.A., Tramontin, A.D., Trevejo, J.M., Herrera, D.G., Garcia-Verdugo, J.M. and Alvarez-Buylla, A. (2000) Noggin Antagonizes BMP Signaling to Create a Niche for Adult Neurogenesis. Neuron 28:713–726.

Makino, S., Fukuda, K., Miyoshi, S., Konishi, F., Kodama, H., Pan, J., Sano, M., Takahashi, T., Hori, S., Abe, H., Hata, J., Umezawa, A. and Ogawa, S. (1999) Cardiomyocytes can be generated from marrow stromal cells in vitro. J Clin Invest 103:697–705.

Marusich, M.F., Furneaux, H.M., Henion, P.D., Weston, J.A. (1994) Hu neuronal proteins are expressed in proliferating neurogenic cells. J Neurobiol 25: 143–155.

Metcalf, D. (1985) The granulocyte-macrophage colony stimulating factors. Cell 43:5–6.

Mezey, E., Chandross, K.J., Harta, G., Maki, R.A. and McKercher, S.R. (2000) Turning blood into brain: cells bearing neuronal antigens generated in vivo from bone marrow. Science 290:1779–1782.

Nakashima, K., Yanagisawa, M., Arakawa, H. and Taga, T. (1999) Astrocyte differentiation mediated by LIF in cooperation with BMP2. FEBS Lett 457:43–46.

Nakashima, K., Takizawa, T., Ochiai, W., Yanagisawa, M., Hisatsune, T., Nakafuku, M., Miyazono, K., Kishimoto, T., Kageyama, R. and Taga, T. (2001) BMP2-mediated alteration in the developmental pathway of fetal mouse brain cells from neurogenesis to astrocytogenesis Proc Natl Acad Sci USA 98:5868–5873.

Petersen, B.E., Bowen, W.C., Patrene, K.D., Mars, W.M., Sullivan, A.K., Murase, N., Boggs, S.S., Greenberger, J.S. and Goff, J.P. (1999) Bone marrow as a potential source of hepatic oval cells. Science 284:1168–1170.

Pincus, D.W., Keyoung, H.M., Harrison-Restelli, C., Goodman, R.R., Fraser, R.A., Edgar, M., Sakakibara, S., Okano, H., Nedergaard, M. and Goldman, S.A. (1998) Fibroblast growth factor-2/brain-derived neurotrophic factor-associated maturation of new neurons generated from adult human subependymal cells. Ann Neurol 43:576–585.

Pittenger, M.F., Mackay, A.M., Beck, S.C., Jaiswal, R.K., Douglas, R., Mosca, J.D., Moorman, M.A., Simonetti, D.W., Craig, S. and Marshak, D.R. (1999) Multilineage potential of adult human mesenchymal stem cells. Science 284:143–147.

Pittenger, M.F., Mosca, J.D., McIntosh, K.R. (2000) Human mesenchymal stem cells: progenitor cells for cartilage bone, fat and stroma. Curr Top Microbiol Immunol 251:3–11.

Ribera, A.B. (1999) Potassium currents in developing neurons. Ann NY Acad Sci 868:399–405.

Ribera, A.B., Spitzer, N.C. (1992) Developmental regulation of potassium channels and the impact on neuronal differentiation. Ion Channels 3:1–38.

Rickard, D.J., Sullivan, T.A., Shenker, B.J., Leboy, P.S. and Kazhdan, I. (1994) Induction of rapid osteoblast differentiation in rat bone marrow stromal cell cultures by dexamethasone and BMP-2. Dev Biol 161:218–228.

Roberts, R., Gallagher, J., Spooncer, E., Allen, T.D., Bloomfield, F. and Dexter, T.M. (1988) Heparan sulphate bound growth factors: a mechanism for stromal cell mediated haemopoiesis. Nature 332:376–378.

Roy, N.S., Wang, S., Jiang, L., Kang, J., Benraiss, A., Harrison-Restelli, C., Fraser, R.A., Couldwell, W.T., Kawaguchi, A., Okano, H., Nedergaard, M. and Goldman, S.A. (2000) In vitro neurogenesis by progenitor cells isolated from the adult human hippocampus. Nat Med 6:271–277.

Sawamoto, K., Yamamoto, A., Kawaguchi, A., Yamaguchi, M., Mori, K., Goldman, S.A. and Okano, H. (2001) Visualization and direct isolation of neuronal progenitor cells by dual-color flow cytometric detection of fluorescent proteins. J Neurosci Res 65:220–227.

Schinstine, M. and Iacovitti, L. (1997) 5-Azacytidine and BDNF enhance the maturation of neurons derived from EGF-generated neural stem cells. Exp Neurol 144:315–325.

Smith, W.C. and Harland, R.M. (1992) Expression cloning of noggin, a new dorsalizing factor localized to the Spemann organizer in *Xenopus* embryos. Cell 70:829–840.

Sugimoto, T., Umezawa, A. and Hata, J. (1997) Neurogenic potential of Ewing's sarcoma cells. Virchows Arch 430:41–46.

Tonegawa, A. and Takahashi, Y. (1998) Somitogenesis controlled by Noggin. Dev Biol 202:172–182.

Tropepe, V., Hitoshi, S., Sirard, C., Mak, T.W., Rossant, J. and van der Kooy, D. (2001) Direct neural fate specification from embryonic stem cells: a primitive mammalian neural stem cell stage acquired through a default mechanism. Neuron 30:65–78.

Umezawa, A., Harigaya, K., Abe, H. and Watanabe, Y. (1990) Gap-junctional communication of bone marrow stromal cells is resistant to irradiation in vitro. Exp Hematol 18:1002–1007.

Umezawa, A., Maruyama, T., Segawa, K., Shadduck, R.K., Waheed, A. and Hata, J. (1992) Multipotent marrow stromal cell line is able to induce hematopoiesis in vivo. J Cell Physiol 151:197–205.

Umezawa, A., Tachibana, K., Harigaya, K., Kusakari, S., Kato, S., Watanabe, Y. and Takano, T. (1991) Colony-stimulating factor 1 is downregulated during the adipocyte differentiation of H-1/A marrow stromal cells and induced by cachectin/tumor necrosis factor. Mol Cell Biol 11:920–927.

Umezawa, A., Yamamoto, H., Rhodes, K., Klemsz, M.J., Maki, R.A. and Oshima, R.G. (1997) Methylation of an ETS site in the intron enhancer of the keratin 18 gene participates in tissue-specific repression. Mol Cell Biol 17:4885–4894.

Wang, E.A., Rosen, V., D'Alessandro, J.S., Bauduy, M., Cordes, P., Harada, T., Israel, D.I., Hewick, R.M., Kerns, K.M., LaPan, P., et al. (1990) Recombinant human bone morphogenetic protein induces bone formation. Proc Natl Acad Sci USA 87:2220–2224.

Weissman, I.L. (2000) Stem cells: units of development, units of regeneration, and units in evolution. Cell 100:157–168.

Whitlock, C.A. and Witte, O.N. (1982) Long-term culture of B lymphocytes and their precursors from murine bone marrow. Proc Natl Acad Sci USA 79:3608–3612.

Whitlock, C.A. and Witte, O.N. (1987) Long-term culture of murine bone marrow precursors of B lymphocytes. Methods Enzymol 150:275–286.

Zimmerman, L.B., De Jesus-Escobar, J.M. and Harland, R.M. (1996) The Spemann organizer signal noggin binds and inactivates bone morphogenetic protein 4. Cell 86:599–606.

Reprinted from BRITISH JOURNAL OF OPHTHALMOLOGY, October 2001, Vol 85, No 10, p 1237-1243

Light induced apoptosis is accelerated in transgenic retina overexpressing human EAT/mcl-1, an anti-apoptotic bcl-2 related gene

Kei Shinoda, Yu Nakamura, Kenichi Matsushita, Kouji Shimoda, Hajime Okita, Mariko Fukuma, Taketo Yamada, Hisao Ohde, Yoshihisa Oguchi, Jun-ichi Hata, Akihiro Umezawa

Abstract

***Background/aim*—EAT/mcl-1 (EAT), an immediate early gene, functions in a similar way to bcl-2 in neutralising Bax mediated cytotoxicity, suggesting that EAT is a blocker of cell death. The aim of this study was to determine the effect of overexpression of the human EAT gene on light induced retinal cell apoptosis.**

***Methods*—EAT transgenic mice incorporating the EF-1α promoter were utilised, and expression of human EAT was detected by RT-PCR. Light damage was induced by raising mice under constant illumination. Two groups of animals, EAT transgenic mice (n=14) and littermates (n=13), were examined by ERG testing and histopathology at regular time points up to 20 weeks of constant light stimulation. Electrophysiological and histopathological findings were evaluated by established systems of arbitrary scoring as scores 0–2 and scores 0–3, respectively.**

***Results*—The mean score (SD) of ERG response was significantly lower in EAT transgenic mice (0.79 (0.89)) than in littermates (1.69 (0.48)) ($p<0.01$). Although the differences between the two survival curves did not reach statistical significance ($p=0.1156$), the estimated incidence of electrophysiological retinal damage was higher in EAT mice (0.0495/mouse/week; 95% confidence interval (CI) 0.0347–0.0500) than in littermates (0. 0199/mouse/week; 95% CI 0.0035–0.0364). The mean scores (SD) for histopathological retinal degeneration were 2.31 (0.63) in littermates and 1.43 (1.22) in EAT transgenic mice ($p=0.065$). However, Kaplan-Meier curves for histopathological failure in two groups of mice showed that retinal photoreceptor cells were preserved significantly against constant light in the littermate compared with transgenic mice ($p=0.0241$). The estimated incidence of histopathological retinal damage was 0.0042/mouse/week in the littermates (95% CI 0–0.0120) and 0.0419/mouse/week in the EAT mice (95% CI 0.0286–0.0500).**

***Conclusion*—Retinal photoreceptor cell apoptosis under constant light stimulation is likely to be accelerated in transgenic retina overexpressing EAT.**

(*Br J Ophthalmol* 2001;85:1237–1243)

Department of Ophthalmology, Keio University School of Medicine, 35 Shinanomachi, Shinjuku-ku, Tokyo 160-8582, Japan
K Shinoda
Y Nakamura
H Ohde
Y Oguchi

Department of Pathology
K Matsushita
H Okita
M Fukuma
T Yamada
J-i Hata
A Umezawa

Department of Internal Medicine
K Matsushita

Laboratory Animal Center
K Shimoda

Correspondence to:
Akihiro Umezawa, Department of Pathology, Keio University School of Medicine, Shinanomachi, Shinjuku-ku, Tokyo, 160-8582, Japan
umezawa@1985.jukuin.keio.ac.jp

Accepted for publication 5 April 2001

The EAT/mcl-1 (EAT) gene was identified by differential screening of cDNA libraries derived from a human myeloid leukaemia cell line induced to undergo differentiation in culture.[1] Expression of EAT is transiently induced in these leukaemia cells after stimulation with agents that promote terminal differentiation, suggesting that this gene functions as an immediate early gene. The EAT gene is a member of the bcl-2 gene family, because it contains the bcl-2 homology domains 1, 2, 3, and 4.[2-5] bcl-2 related genes have either positive or negative regulatory effects on apoptosis in vitro and in vivo.[6-8] Previous studies have established that Bcl-2, Bcl-xL, Bcl-w, Bfl-1, EAT, and A1 are anti-apoptotic molecules while Bax, Bak, Bcl-xS, Bad, Bid, Bik, and Hrk are pro-apoptotic molecules.[9-19] The rapid increase in expression of EAT produced by differentiating or cytotoxic agents was found to involve an increase in EAT transcription,[20-22] indicating that the EAT early induction gene is similar to the serum stimulated early response genes.[23-28] The EAT protein also exhibits rapid turnover (half life of 1–3 hours)[29] because, unlike other bcl-2 family members, the N-terminal region contains two PEST sequences (enriched in proline, glutamic acid, serine, and threonine). The intracellular distribution of EAT appears to be more widespread than Bcl-2.[30 31]

The in vivo effects of bcl-2 related genes have been investigated in transgenic or knockout mice. bcl-2 transgenic mice increased cell survival of B cells, T cells, and thymocytes.[32-35] Mice deficient for bcl-2 display increased apoptosis in selected tissues.[36] These phenotypes confirm the anti-apoptotic functions established for bcl-2 in vitro. In contrast, bax transgenic mice have increased apoptosis of T cells, whereas mice deficient for bax demonstrate hyperplasia of thymocytes and B cells.[37-39] Male Bax deficient mice are infertile with atrophic adult testes and an empty epididymis and vas deferens; a complete cessation of mature sperm cell production occurs in these mice.[39] These phenotypes result from the pro-apoptotic functions of Bax.

Apoptosis is the main mechanism of cell loss in induced[40 41] or inherited retinal degeneration[42 43] in animal models, and it may represent the mechanism of cell death in many human retinal diseases. The pathogenesis of retinal degeneration is largely unexplained, and there are no current therapies. Excessive light may enhance the progression and severity of human

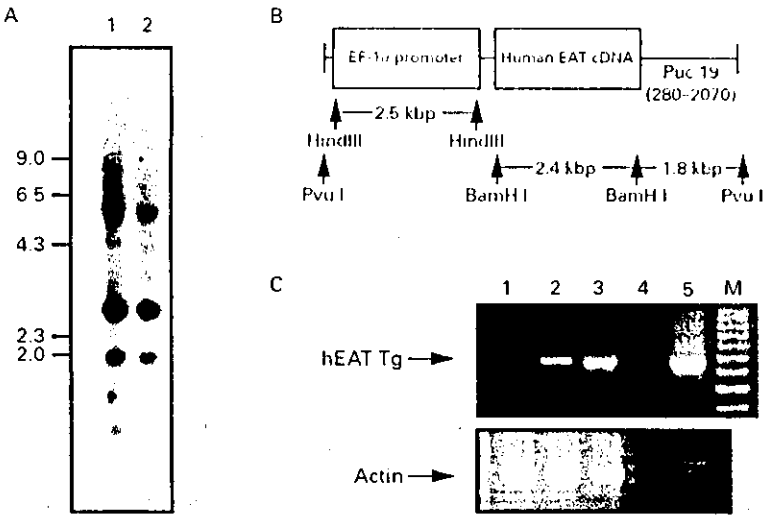

Figure 1 Expression of the human EAT transgene. (A) Southern blot analysis of tail DNA from heterozygote transgenic lines. EcoRI digested tail genomic DNA was hybridised with a ^{32}P labelled EF1α-EAT probe. Kilobase size markers are shown on the left. Orientation of the human EAT transgene was determined to be head to tail in all lines. The copy numbers of the transgene per diploid genome for each line are: 150 (E3), and 20 (E12), as shown in lanes 1 and 2, respectively. To determine the copy number of the transgene, transgene fragment copy numbers were also hybridised. (B) Schema of the EF1α human EAT (EF1α-EAT) transgenic construct. The PvuI fragment was used as the transgene. The same 6.7 kb PvuI fragment was used as a probe for Southern blot hybridisation. This human EAT transgene, driven by the EF-1α promoter, was injected into the fertilised eggs. (C) Expression of the human EAT transgene as assayed in isolated retinas from the transgenic lines. RT-PCR was performed with a primer set which detected only the human EAT gene without detecting the endogenous murine EAT gene (lane 1: non-transgenic mice; lane 2: E12; lane 3: E13; lane 4: no RNA; lane 5: plasmid containing the human EAT gene). Retinas from a non-transgenic mouse and the human EAT DNA served as negative and positive controls, respectively. A 100 bp ladder is shown as a size marker in lane M. β actin (729 bp) RT-PCR products are shown to demonstrate the integrity of the isolated RNA (lower section).

age related macular degeneration and some forms of retinitis pigmentosa.[17 18] Animal models of light induced retinal degeneration correlate well with the pathology observed in human donor retinas affected with retinitis pigmentosa.[17 18] In addition, apoptosis in photoreceptor (PR) cells has been seen in early stages of human retinitis pigmentosa.[19] Likewise, several animal models with inherited retinal degeneration show an increased susceptibility to light damage compared with control animals.[20] Exposure to excessive levels of white light induces PR apoptosis, thus providing an excellent model to analyse degenerative PR loss.[21]

PRs overexpressing bcl-2 have been shown to survive light induced insults longer than PRs with normal endogenous levels of bcl-2.[22] Expression of bcl-2 protects against PR degeneration in retinal degeneration slow (rds) mice.[23 24] Increased expression of bcl-2 and bcl-xL may be a necessary component in a strategy to inhibit PR cell death. These findings led us to examine the effect of overexpression of the human EAT gene on light induced retinal cell apoptosis.

Materials and methods

MICE TRANSGENIC FOR HUMAN EAT GENE

To generate transgenic mice that express human EAT, a transgene was constructed with the human EF-1α promoter linked to human EAT (EF1α-EAT)[25] (Fig 1). A DNA solution (3 μg/ml) was microinjected into the male pronuclei of fertilised mouse eggs taken from superovulated B6C3F1 (C57BL/6 × C3H/He) females. The injected eggs were surgically transferred to the oviducts of B6C3F1 pseudopregnant female mice. Transgene bearing mice were selected by Southern blot analysis of tail DNA (10 μg) hybridised with the EF1α-EAT probe of the 6.7 kb PvuI-PvuI fragment. The founder mice obtained were assigned a number preceded with a letter E for example, E3 or E12. Offspring were screened by detecting the 1097 bp human EAT fragment in the tail DNA by polymerase chain reaction (PCR) using a set of appropriate primers. The sequences of the primers used were as follows; sense, 5' CTGCATCGAACCATTAGCAG 3', antisense, 5' TACAACCAGTCTGCATACAG 3'.

C3H/He and C57BL/6 mice, which are pigmented, were purchased from Clea Japan (Tokyo, Japan). All mice were maintained in our animal facility under specific pathogen-free conditions. The mice were housed under a controlled photoperiod (12 hours of light, 12 hours of darkness) and temperature (22–25°C) and given water and chow ad labium in cages. The study was approved by the Keio University, School of Medicine, Laboratory Animal Care and Use Committee (No 001106).

SOUTHERN BLOT ANALYSIS

For Southern blot analysis, 5 μg of total genomic DNA was digested to completion with *Eco*RI, separated by 0.8% agarose gel electrophoresis, and transferred to Hybond N+ filters (Amersham, UK) in 1.5 M NaCl/0.25 N NaOH (Fig 1A). The membranes were prehybridised at 65°C for 3 hours in 5 × SSPE (1 × SSPE = 0.15 M NaCl, 1 mM EDTA and 0.01 M sodium phosphate buffer), 5 × Denhardt's solution, 1% SDS, and 10 μg of poly A/ml, and then hybridised with the *Bam*HI fragment of human EAT cDNA (2.4 kb) labelled with [α-^{32}P]-dCTP by the random primer method at 1–3 × 10^9 cpm/μg of specific activity.[26] After overnight hybridisation , blots were washed twice with 1 × SSPE, 1% SDS at room temperature, twice with 1 × SSPE, 1% SDS at 65°C, and twice with 0.1 × SSPE, 0.1% SDS at 65°C, and then exposed to *x* ray film.

EXPRESSION OF HUMAN EAT IN TRANSGENIC MICE

Expression of human EAT transgene in the mice was examined by reverse transcription and polymerase chain reaction (RT-PCR). Briefly, retina from the mice were snap frozen in liquid nitrogen and homogenised in a microcentrifuge tube. RNA was extracted from these samples by Isogen (Nippon Gene, Japan). To eliminate the possibility of genomic DNA contamination, the RNA samples were further treated with RNase-free DNase and RNase inhibitor at 37°C for 1 hour followed by ethanol precipitation with the use of tRNA as a carrier. Complementary DNA was generated using a first strand cDNA synthesis kit (Pharmacia Biotech, Uppsala, Sweden) and used as a template for PCR. Approximately 1–5 μg of total RNA was transcribed. PCR was carried out in 100 μl reactions containing 1–7 μl cDNA template, 200 mM deoxynucleotide triphosphates, 0.5 mM of each oligonucleotide primer, and 2.5 units of Taq polymerase in 10

mM TRIS HCl buffer, pH 8.8, containing 50 mM KCl, 1.5 mM MgCl. Oligonucleotide primers used for PCR were: 5'-CTGCATCGAACCATTAGCAG (sense) and 5'-TACAACCAGTCTGCATACAG (antisense). They were used to amplify a 1097 bp fragment of human EAT cDNA without detecting the endogenous murine EAT gene. The PCR reaction was performed for 35 cycles with the following parameters: denaturing at 95°C for 1 minute, annealing at 55°C for 1 minute, and elongation at 72°C for 90 seconds. The amplified PCR products were electrophoresed on 0.7% agarose gels and either detected by ultraviolet illumination of ethidium bromide stained gels or transferred to filter and hybridised with ^{32}P labelled EAT cDNA as a probe.

Two lines (E13 and E12) of EAT transgenic mice incorporating the EF-1α promoter were utilised. Expression of human EAT was detected by RT-PCR in transgenic mice. Northern blot analysis of various tissues was initially carried out on both lines of transgenic mice to detect human EAT mRNA; however, no signals could be detected. Western blots using an EAT specific monoclonal antibody and a polyclonal antibody were likewise carried out on both lines to detect expression of human EAT protein; however, detectable levels of human EAT could not be observed. In vitro, cells transfected with the same transgene constructs have previously been shown to express the EAT protein by western blot analysis,[7] confirming the integrity of these constructs. Expression of the EAT gene in various organs, as examined by RT-PCR (Fig 1C) revealed ubiquitous expression of EAT in transgenic mice. Strong expression of the transgene was noted in the retina. We concluded that the use of the EF-1α promoter

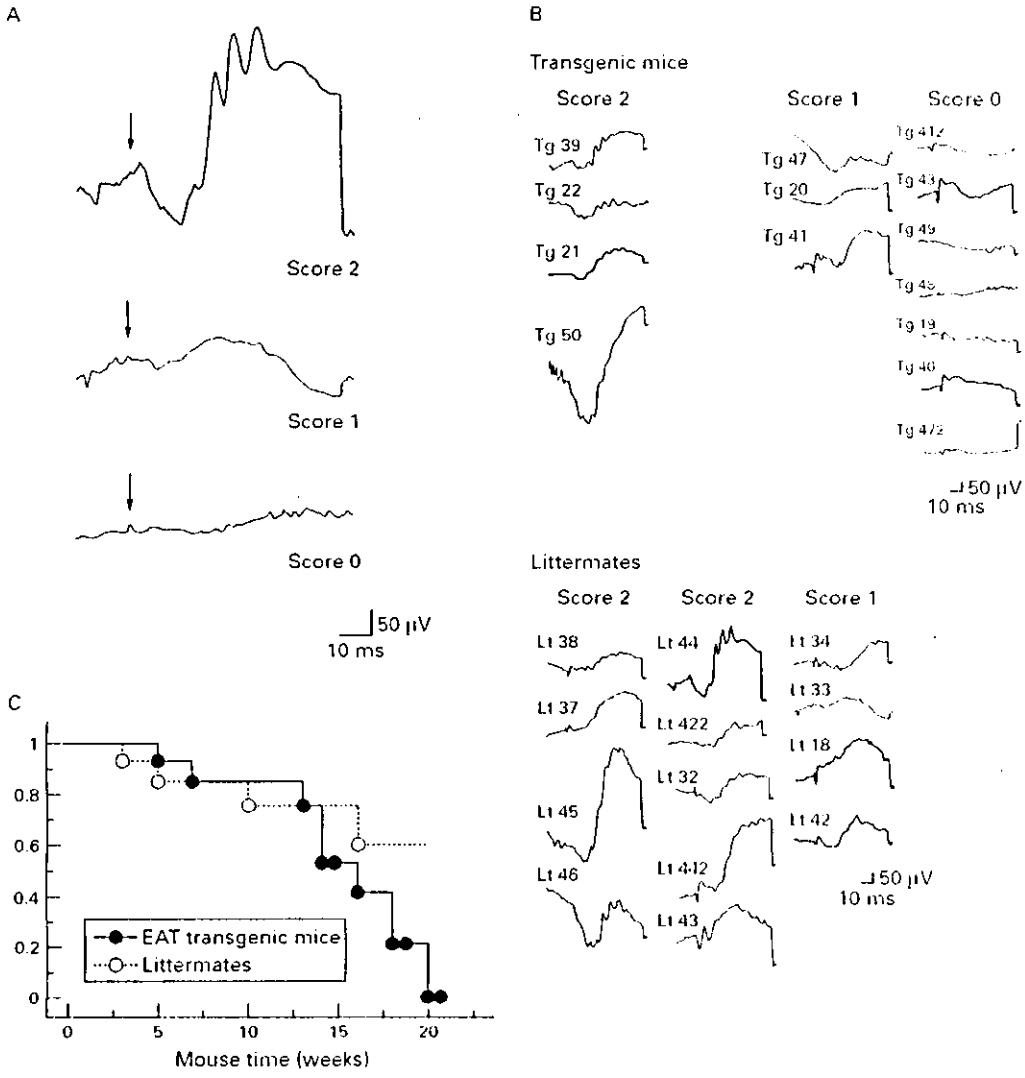

Figure 2 Electroretinograms of mice in which light damage was induced by constant light stimulation. (A) The ERG responses were scored by three observers unaware of the EAT genotype for the degree of potential rescue. The scores were based on scale 0 (severe damage with little or no rescue; almost non recordable), 1 (little damage; a-wave and b-wave seen without oscillatory potentials), and 2 (no damage; a, b-wave amplitude and oscillatory potentials well preserved). Arrows indicate the point of light stimulation. (B) The ERG responses of each mouse. Mice were raised under cyclic room lighting until 55–91 days of age and then were placed in a temperature controlled environmental chamber illuminated continuously by 20 white fluorescent bulbs (40 W). The illumination in the chamber ranged from 400 to 500 lux. (C) Kaplan-Meier survival analysis of electrophysiological responses after constant light stimulation in EAT transgenic mice (solid circle) and littermates (open circle). Criteria for success and failure are described in the Materials and methods section. The estimated incidence of electrophysiological retinal damage was 0.015 per week in littermates, and 0.005 per week in EAT transgenic mice.

resulted in expression of EAT transgene at levels detectable by RT-PCR.

INDUCTION OF LIGHT DAMAGE

As described by Lavail *et al*, mice were raised under cyclic room lighting until 5–13 weeks of age and then were placed in a temperature controlled environmental chamber illuminated continuously by 26 white fluorescent bulbs (40 W). Light intensity in the cages ranged from 400 to 500 lux. Groups of animals were examined by electroretinogram (ERG) testing after 3, 5, 7, 9, 10, 13, 14, 16, 18, or 20 weeks in constant lighting, and then killed and tissues were taken for histology. The number of mice examined in each group was as follows: non-transgenic (littermate) at 3 weeks, n = 1; at 5 weeks, n = 1; at 7 weeks, n = 1; at 9 weeks, n = 1; at 10 weeks, n = 1; at 13 weeks, n = 2; at 14 weeks, n = 1; at 16 weeks, n = 1; at 18 weeks, n = 2; at 20 weeks, n = 2; and EAT transgenic at 3 weeks, n = 1; at 5 weeks, n = 1; at 7 weeks, n = 1; at 9 weeks, n = 1; at 10 weeks, n = 1; at 13 weeks, n = 2; at 14 weeks, n = 2; at 16 weeks, n = 1; at 18 weeks, n = 2; at 20 weeks, n = 2.

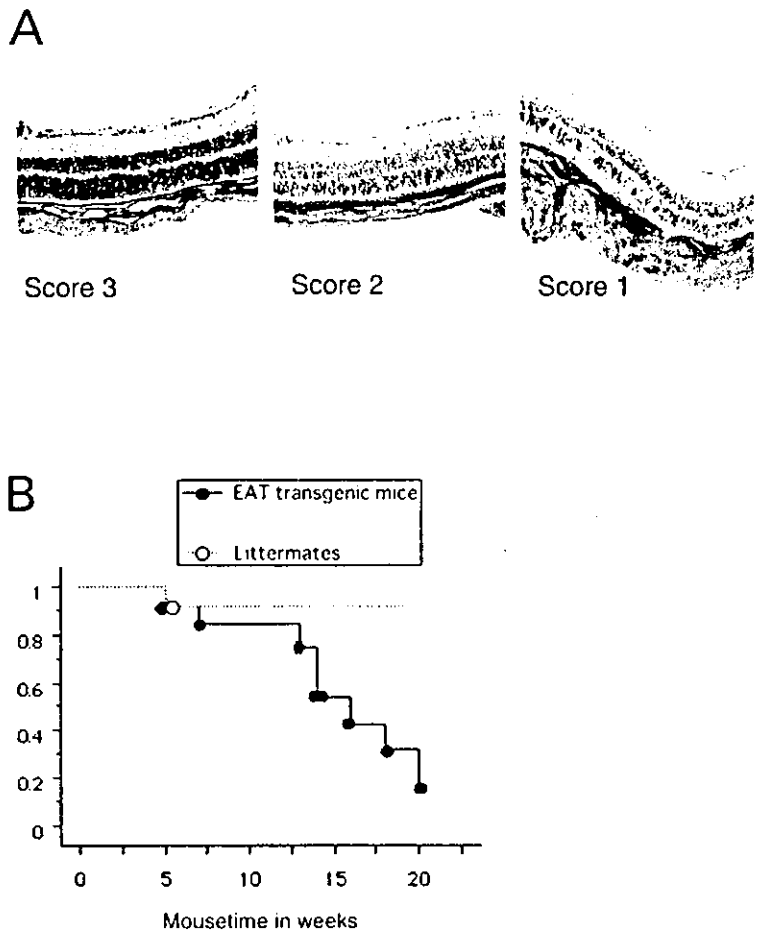

Figure 3 Light micrographs of mouse retinas taken from the posterior to equatorial region in the superior hemisphere of the eye. (A) Histological sections cut along the vertical meridian were scored by three observers for the degree of potential rescue, since the region is most sensitive to the damaging effects of constant light. The scores were: score 1 (the outer nuclear layer (ONL) has been reduced to about 3–5 rows of nuclei; disorganised inner segment (IS) and outer segment (OS) are still present), score 2 (photoreceptor IS and some disorganised OS are still present; the ONL still consists of approximately 6–8 rows of nuclei) and score 3 (almost normal structure with 9–10 rows of photoreceptor nuclei comprising the ONL). (B) Kaplan-Meier survival analysis of histopathological findings of the retina after constant light stimulation in the EAT transgenic mice (solid circle) and littermate (open circle). Criteria for success and failure are described in the Materials and methods section. The estimated incidence of histopathological retinal damage was 0.0042 mouse/week in the littermates and 0.0419 mouse/week in the EAT transgenic mice.

ELECTROPHYSIOLOGICAL STUDY

Mice were dark adapted for 12 hours before ERG testing as described. Anaesthesia was performed with inhalation of diethyl ether, and the anaesthetised animal was placed on a heating pad (37°C). Pupils were dilated by 0.5% tropicamide. A corneal electrode, which was made from gold, instead of an intravitreous electrode, was used for recording. The ground electrodes were attached subcutaneously in the neck. A 26 gauge needle was placed subcutaneously in the head as a reference electrode. All manipulations were performed under very dim red light. Full field ERGs were elicited with 10 μs flashes of xenon light (20 J) from a Ganzfeld dome on a steady background of 0 cd/m^2. Responses were differentially amplified at a gain of 10 000. Analysis time was 100 ms. Single flash response was recorded. Four or eight flash responses were averaged if it was noisy. Flashes were presented at a rate of about 0.3 Hz manually. The recording band pass was 0.5–100 Hz. The ERG measurements were all made by the investigators blinded to the genotypes of the mice.

The ERG responses were scored by three observers masked with respect to the EAT genotype for the degree of potential rescue. The scores were defined as follows (Fig 2A): score 0, severe damage with little or no rescue, almost non-recordable; score 1, little damage, a and b-waves observed without oscillatory potentials; score 2, no damage, a, b-wave amplitude and oscillatory potentials well preserved.

Criteria for success were defined as good preservation of the oscillatory potentials that is, scores of 0 or 1 were considered failure. Data were analysed statistically using Kaplan-Meier survival analysis with Mantel-Cox log rank test for estimation of success.

HISTOPATHOLOGICAL STUDY

After ERG recordings following a rigid protocol, the anaesthetised animals were killed by cervical dislocation, and the eyes were processed for histology. After fixation for 1–2 days, the posterior segment containing the retina could be sectioned along the vertical meridian. Sections (6 μm thick) were processed and stained with haematoxylin and eosin.

Histological sections cut along the vertical meridian were scored by three observers for the degree of potential rescue. The scores were defined as follows (Fig 3A): score 0, severe damage with little or no rescue, all photoreceptor inner segment (IS) and outer segment (OS) missing, and the outer nuclear layer (ONL) reduced to less than a single or two rows of photoreceptor nuclei; score 1, moderate damage, the ONL has been reduced to about 3–5 rows of nuclei; disorganised IS and OS are still present; score 2, little damage, photoreceptor IS and some disorganised OS are still present, the ONL still consists of approximately 6–8 rows of nuclei; and score 3, no damage, almost normal structure remained with 9–10 rows of

photoreceptor nuclei comprising the ONL. The scores were done with the observers unaware of the EAT genotype and were based on ONL thickness in different regions of the eye as well as PR inner and outer segment length and integrity.

Criteria for success were defined as at least 3–5 rows of nuclei in ONL, where a score of 0 or 1 was considered failure. Data were analysed statistically using Kaplan-Meier survival analysis with Mantel-Cox log rank test for estimation of success. Statistical significance was set at 0.05.

Results

We used ERG to estimate retinal function in mice carrying an EAT transgene under the EF-1α promoter. Light damage was induced in mice by constant illumination. EAT transgenic mice (n = 14) and control littermates (n = 13) were examined by ERG testing at various time points to 20 weeks of constant lighting stimulation. The ERG response score is shown in Table 1A. The mean scores (SD) of ERG dysfunction were significantly lower ($p < 0.01$) in the EAT transgenic mice (0.79 (0.89)) than the littermates (1.69 (0.48)). In addition, Kaplan-Meier curves showed a greater decline in electrophysiological response due to constant light in EAT transgenic mice than in littermates (Fig 2C). The estimated incidence of electrophysiological retinal damage was 0.0199/mouse/week (95% CI 0.0035-0.0364) in the littermate and 0.0495/mouse/week in the EAT transgenic mice (95% CI 0.0347–0.0500). The ERG responses of the retina deteriorated more markedly in the transgenic mice than in the littermates ($p = 0.1156$, Kaplan-Meier survival analysis with Mantel-Cox log rank test), suggesting that PR apoptosis under the constant light stimulation is likely to be accelerated by EAT (Fig 2B, C).

To determine whether this retinal dysfunction is caused by cell death or degeneration, we examined all retinas histopathologically. The results clearly showed that the electrophysiological disturbance was caused by loss of retinal cells. Histopathology scores are shown in Table 1B. There was a trend towards lower mean scores (SD) of histopathological change in the EAT transgenic mice (1.43 (1.22)) than in littermates (2.31 (0.63)) ($p = 0.065$). The estimated incidence of histopathological retinal damage was 0.0012/mouse/week in littermates (95% CI 0-0.0120) and 0.0419/mouse/week in the EAT transgenic mice (95% CI 0.0286–0.0500). Retinal PR cells were significantly more impaired by constant light in the EAT transgenic mice than the littermate (Fig 3B, $p = 0.0241$, Kaplan-Meier survival analysis with Mantel-Cox log rank test), implying that dysfunction detected by ERG is attributable to retinal cell death.

Table 1 The ERG responses and histopathological findings of mice retina exposed to constant light stimulation

		Score			
A	*Genotype*	*0*	*1*	*2*	*Total*
	Transgenic	7	3	4	14
	Littermate	0	4	9	13

		Score				
B	*Genotype*	*0*	*1*	*2*	*3*	*Total*
	Transgenic	4	4	2	4	14
	Littermate	0	1	7	5	13

The ERG responses and histopathological findings were scored by three observers blinded to the EAT genotype for the degree of potential rescue. Definition of the scores are described in the Materials and methods section. (A) The mean score (SD) of the ERG response of EAT transgenic mice (0.79 (0.89)) was significantly lower than that of the littermates (1.69 (0.48)), $p = 0.0074$). (B) The mean scores (SD) of the histopathological findings of the littermates (2.31 (0.63)) versus EAT transgenic mice (1.43 (1.22)) were not significantly different ($p = 0.065$).

Discussion

Light induced apoptosis of retinal PRs has been well characterised, but the receptor mediating light damage has not yet been identified.[11] Candidate molecules include prostaglandin synthase,[58] cytochrome oxidase,[59] rhodopsin,[60] and opsins of the cones and the retinal pigment epithelium.[61] c-fos, a transcription factor and a component of AP-1, has been reported to be essential for a specific premitochondrial "private apoptotic pathway" induced by light.[62] In the present study, we have shown that retinal cell death by light was accelerated by EAT, a bcl-2 related gene, using EAT transgenic mice.

The proto-oncogene bcl-2 and its family, which are known to be potent regulators of apoptosis, have attracted great attention in light induced apoptosis (Fig 4). However, little remains known about their role. Chen *et al* reported that bcl-2 overexpression reduces PRs apoptosis against sustained illumination.[52] However, Joseph and Li reported that the outer layer thickness in bcl-2 or bcl-xL transgenic retinas was not significantly different from non-transgenic ones after exposure to excessive light stimulation.[54] This is explained by the presence of multiple pathways of cell death in PRs that bypass regulation by bcl-2 family proteins.

Similar to bcl-2, EAT has been shown to inhibit apoptosis in vitro and in vivo.[57 63 64] The ratio of anti-apoptotic (death antagonists) to pro-apoptotic bcl-2 related molecules (death agonists) is known to determine whether a cell will undergo apoptosis. This death-life balance is regulated partly by competitive dimerisation between pairs of antagonists and agonists[2] (Fig 4). Similar to bcl-2, EAT may heterodimerise with Bax through BH1 and BH2 domains to repress apoptosis.[18 65 66] The interactions of EAT with Bax are more physiologically relevant in cells that fail to express bcl-2, as the bax gene is more widely expressed than bcl-2.[67] The current study is, to our knowledge, the first report to investigate the role of EAT in regulation of retinal PR cell death. The estimated incidence of electrophysiological and morphological retinal damage was increased by EAT.

There were five mice (Tg 41, Tg 472, Lt 34, Lt 18, and Lt 42) defined as "failure" in the electrophysiological study but as "success" in the histopathological findings. There was, however, no mouse defined as "success" in the electrophysiological study and as "failure" in

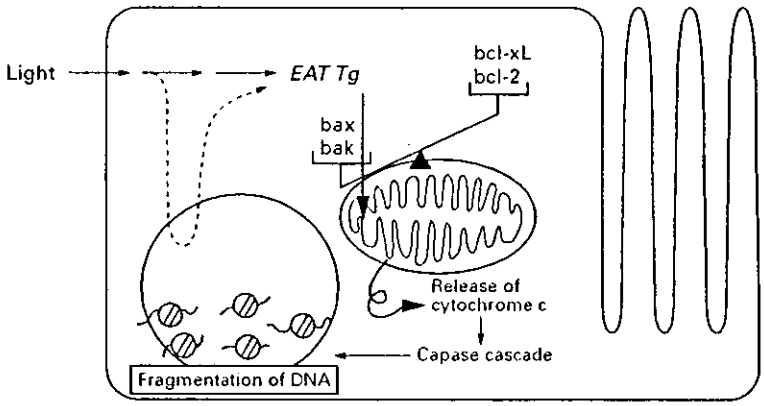

Figure 4 Schematic model of the mechanism of EAT transgene incorporation in promoting light induced apoptosis in the retina. Light triggers a signal cascade mechanism which initiates the apoptotic signal through activation of the JNK (SAPK) pathways and/or c-fos (AP-1) transcriptional pathways. EAT and other Bcl-2 related proteins act at the outer membrane of the mitochondria[70] where the heterodimeric balance of bcl-2 related genes regulates the final execution stages of the apoptotic cascade. Bcl-2 related genes regulate mitochondrial membrane function; a loss in mitochondrial transmembrane potential leads to the release of AIF and cytochrome c. These factors then trigger apoptosis in which the caspase activated cascade leads to the activation of endonucleases resulting in DNA fragmentation. We hypothesise that incorporation of the EAT transgene shifts the balance of bcl-2 related heterodimeric molecules in the direction of promoting apoptotic effector signals. EAT promotes light induced apoptosis in retina by the above mechanism.

the histopathological findings. These results indicate that the electrophysiological response was more sensitive than histopathology for the evaluation of retinal cell apoptosis in the present study. The functional consequences of this degeneration seem to have a more rapid course of deterioration than do the histopathological ones. This is consistent with a previous report showing the retardation of PR degeneration in $Pde^{rd1}/Pdeg^{rd1}$ mice by the bcl-2 transgene,[46] in which although both cell types were protected from cell death on microscopic examination, only the cone cells were functional, and not the rod cells, in signal transduction in ERG analysis.

There are two possible roles of EAT in cells exposed to cytotoxic agents.[20] One possibility is that the rapid increase in EAT might provide an initial viability enhancing or death delaying response. In such cases, EAT might serve an anti-apoptotic function and might allow cells a margin of time to respond to the cytotoxic stimulus (for example, time to decide either to undergo apoptosis or to initiate further measures to prevent cell death). The other possibility is that EAT might have an as yet unproved dual role in the control of cell viability (as is seen with bax and bcl-xL, another member of the bcl-2 family)[69 70] and might in some way contribute to the death that follows increased EAT expression. In the current study, the observation that light induced apoptosis was accelerated in transgenic retina overexpressing EAT supports the latter hypothesis that anti-apoptotic Bcl-2 and Bcl-xL can convert into pro-apoptotic proteins.[71 72] Structural data indicate that the cleavage of Bid, a Bcl-2 related protein, by caspase-8 induces a conformational change that may facilitate exposure of its BH3 domain.[71 73] The BH3 domain may be involved in triggering death, and is conserved in Bax, EAT, Bcl-2, and Bcl-xL.[72] Perhaps like Bcl-2, EAT functions as an anti-apoptotic protein that can be converted into a pro-apoptotic protein by alternative splicing, phosphorylation, proteolytic cleavage, or relocalisation. The potential role of these factors in the chain of events leading to PRs cell death in the retina remains to be investigated. Elucidation of the apoptotic pathway in EAT transgenic mice may lead to identification of other factors that interfere with cell death and of molecular therapeutic strategies that might prevent retinal degeneration.

The first two authors contributed equally to this work.

We are grateful to K Kita, J Ozawa, H Suzuki, S Kusakari, H Abe, Y Hashimoto, and T Honda for their technical assistance. This work was supported in part by a grant from the ministry of education, science and culture to JH and AU, by Keio University special grant in aid for innovative collaborative research project to JH and AU, by Keio Gijuku Fukuzawa memorial funds for the advancement of education and research from Keio University to HO, and by a national grant in aid for the establishment of a high tech research centre at private universities.

1 Kozopas KM, Yang T, Buchan HL, *et al.* MCL1, a gene expressed in programmed myeloid cell differentiation, has sequence similarity to BCL2. *Proc Natl Acad Sci USA* 1993;90:3516–20.
2 Kroemer G. The proto-oncogene Bcl-2 and its role in regulating apoptosis. *Nat Med* 1997;3, 614–20.
3 Revilla Y, Cebrian A, Baixeras E, *et al.* Inhibition of apoptosis by the African swine fever virus Bcl-2 homologue: role of the BH1 domain. *Virology* 1997;228:400–4.
4 Umezawa A, Maruyama T, Inazawa J, *et al.* Induction of mcl1/EAT, Bcl-2 related gene, by retinoic acid or heat shock in the human embryonal carcinoma cells, NCR-G3. *Cell Struct Funct* 1996;21:143–50.
5 Okita H, Umezawa A, Suzuki A, *et al.* Up-regulated expression of murine Mcl1/EAT, a bcl-2 related gene, in the early stage of differentiation of murine embryonal carcinoma cells and embryonic stem cells. *Biochim Biophys Acta* 1998; 1398:335–41.
6 Reed JC. Bcl-2 and the regulation of programmed cell death. *J Cell Biol* 1994;124:1–6.
7 Reed JC. Mechanisms of Bcl-2 family protein function and dysfunction in health and disease. *Behring Inst Mitt* 1996;97:72–100.
8 Reed JC. Balancing cell life and death: bax, apoptosis, and breast cancer. *J Clin Invest* 1996;97:2405–4.
9 Boise LH, Gonzalez-Garcia M, Postema CE, *et al.* bcl-x, a bcl-2-related gene that functions as a dominant regulator of apoptotic cell death. *Cell* 1993;74:597–608.
10 Boyd JM, Gallo GJ, Elangovan B, *et al.* Bik, a novel death-inducing protein shares a distinct sequence motif with Bcl-2 family proteins and interacts with viral and cellular survival-promoting proteins. *Oncogene* 1995;11:1921–8.
11 Chittenden T, Harrington EA, O'Connor R, *et al.* Induction of apoptosis by the Bcl-2 homologue Bak. *Nature* 1995;374:733–6.
12 D'Sa-Eipper C, Subramanian T, Chinnadurai G. bfl-1, a bcl-2 homologue, suppresses p53-induced apoptosis and exhibits potent cooperative transforming activity. *Cancer Res* 1996;56:3879–82.
13 Gibson L, Holmgreen SP, Huang DC, *et al.* Bcl-w, a novel member of the bcl-2 family, promotes cell survival. *Oncogene* 1996;13:665–75.
14 Inohara N, Ding L, Chen S, *et al.* Harakiri, a novel regulator of cell death, encodes a protein that activates apoptosis and interacts selectively with survival-promoting proteins Bcl-2 and Bcl-X(L). *Embo J* 1997;16:1686–94.
15 Lin EY, Orlofsky A, Wang HG, *et al.* A1, a Bcl-2 family member, prolongs cell survival and permits myeloid differentiation. *Blood* 1996;87:983–92.
16 Thompson CB. Apoptosis in the pathogenesis and treatment of disease. *Science* 1995;267:1456–62.
17 Yang E, Korsmeyer SJ. Molecular thanatopsis: a discourse on the BCL2 family and cell death. *Blood* 1996;88:386–401.
18 Yang E, Zha J, Jockel J, *et al.* Bad, a heterodimeric partner for Bcl-XL and Bcl-2, displaces Bax and promotes cell death. *Cell* 1995;80:285–91.
19 Moulding DA, Giles RV, Spiller DG, *et al.* Apoptosis is rapidly triggered by antisense depletion of MCL-1 in differentiating U937 cells. *Blood* 2000;96:1756–63.
20 Yang T, Buchan HL, Townsend KJ, *et al.* MCL-1, a member of the BCL-2 family, is induced rapidly in response to signals for cell differentiation or death, but not to signals for cell proliferation. *J Cell Physiol* 1996;166:523–36.
21 Matsushita K, Umezawa A, Iwanaga S, *et al.* The EAT mcl-1 gene, an inhibitor of apoptosis, is up-regulated in the early stage of acute myocardial infarction. *Biochim Biophys Acta* 1999;1472:471–8.
22 Wakabayashi K, Saito H, Ebinuma H, *et al.* Bcl-2 related proteins are dramatically induced at the early stage of differentiation in human liver cancer cells by a histone deacetylase inhibitor projecting an anti-apoptotic role during this period. *Oncol Rep* 2000;7:285–8.
23 Christy BA, Lau LF, Nathans D. A gene activated in mouse 3T3 cells by serum growth factors encodes a protein with

zinc finger sequences. *Proc Natl Acad Sci USA* 1988;85: 7857–61.
21 Lau LF, Nathans D. Expression of a set of growth-related immediate early genes in BALB/c 3T3 cells: coordinate regulation with c-fos or c-myc. *Proc Natl Acad Sci USA* 1987;84:1182–6.
25 Reed JC, Tsujimoto Y, Alpers JD, *et al.* Regulation of bcl-2 proto-oncogene expression during normal human lymphocyte proliferation. *Science* 1987;236:1295–9.
26 Ryder K, Nathans D. Induction of protooncogene c-jun by serum growth factors. *Proc Natl Acad Sci USA* 1988;85: 8464–7.
27 Akgul C, Turner PC, White MR, *et al.* Functional analysis of the human MCL-1 gene. *Cell Mol Life Sci* 2000;57:684–91.
28 Moulding DA, Quayle JA, Hart CA, *et al.* Mcl-1 expression in human neutrophils: regulation by cytokines and correlation with cell survival. *Blood* 1998;92:2495–502.
29 Yang T, Kozopas KM, Craig RW. The intracellular distribution and pattern of expression of Mcl-1 overlap with, but are not identical to, those of Bcl-2. *J Cell Biol* 1995;128: 1173–84.
30 Sano M, Umezawa A, Suzuki A, *et al.* Involvement of EAT/mcl-1, an anti-apoptotic bcl-2-related gene, in murine embryogenesis and human development. *Exp Cell Res* 2000;259:127–39.
31 Suzuki A, Umezawa A, Sano M, *et al.* Involvement of EAT/mcl-1, a bcl-2 related gene, in the apoptotic mechanisms underlying human placental development and maintenance. *Placenta* 2000;21:177–83.
32 McDonnell TJ, Deane N, Platt FM, *et al.* bcl-2-immunoglobulin transgenic mice demonstrate extended B cell survival and follicular lymphoproliferation. *Cell* 1989; 57:79–88.
33 Sentman CL, Shutter JR, Hockenbery D, *et al.* bcl-2 inhibits multiple forms of apoptosis but not negative selection in thymocytes. *Cell* 1991;67:879–88.
34 Siegel RM, Katsumata M, Miyashita T, *et al.* Inhibition of thymocyte apoptosis and negative antigenic selection in bcl-2 transgenic mice. *Proc Natl Acad Sci USA* 1992;89: 7003–7.
35 Strasser A, Harris AW, Cory S. bcl-2 transgene inhibits T cell death and perturbs thymic self- censorship. *Cell* 1991; 67:889–99.
36 Veis DJ, Sorenson CM, Shutter JR, *et al.* Bcl-2-deficient mice demonstrate fulminant lymphoid apoptosis, polycystic kidneys, and hypopigmented hair. *Cell* 1993;75:229–40.
37 Brady HJ, Salomons GS, Bobeldijk RC, *et al.* T cells from baxalpha transgenic mice show accelerated apoptosis in response to stimuli but do not show restored DNA damage-induced cell death in the absence of p53. gene product in. *Embo J* 1996;15:1221–30.
38 Brady HJ, Gil-Gomez G, Kirberg J, *et al.* Bax alpha perturbs T cell development and affects cell cycle entry of T cells. *Embo J* 1996;15:6991–7001.
39 Knudson CM, Tung KS, Tourtellotte WG, *et al.* Bax-deficient mice with lymphoid hyperplasia and male germ cell death. *Science* 1995;270:96–9.
40 Abler AS, Chang CJ, Ful J, *et al.* Photic injury triggers apoptosis of photoreceptor cells. *Res Commun Mol Pathol Pharmacol* 1996;92:177–89.
41 Hafezi F, Marti A, Munz K, *et al.* Light-induced apoptosis: differential timing in the retina and pigment epithelium. *Exp Eye Res* 1997;64:963–70.
42 Portera-Cailliau C, Sung CH, Nathans J, *et al.* Apoptotic photoreceptor cell death in mouse models of retinitis pigmentosa. *Proc Natl Acad Sci USA* 1994;91:974–8.
43 Reme CE, Grimm C, Hafezi F, *et al.* Apoptotic cell death in retinal degenerations. *Prog Retin Eye Res* 1998;17:443–64.
44 Cruickshanks KJ, Klein R, Klein BE. Sunlight and age-related macular degeneration. The Beaver Dam Eye Study. *Arch Ophthalmol* 1993;111:514–8.
45 Simons K. Artificial light and early-life exposure in age-related macular degeneration and in cataractogenic phototoxicity [letter; comment]. *Arch Ophthalmol* 1993; 111:297–8.
46 Cideciyan AV, Hood DC, Huang Y, *et al.* Disease sequence from mutant rhodopsin allele to rod and cone photoreceptor degeneration in man. *Proc Natl Acad Sci USA* 1998;95: 7103–8.
47 Flannery JG, Farber DB, Bird AC, *et al.* Degenerative changes in a retina affected with autosomal dominant retinitis pigmentosa. *Invest Ophthalmol Vis Sci* 1989;30: 191–211.
48 Li ZY, Jacobson SG, Milam AH. Autosomal dominant retinitis pigmentosa caused by the threonine-17-methionine rhodopsin mutation: retinal histopathology and immunocytochemistry. *Exp Eye Res* 1994;58:397–408.
49 Li ZY, Milam AH. In: Anderson RE, LaVail MM, Hollyfield JG, eds. *Degenerative disease of the retina.* New York: Plenum, 1995:1–8.
50 LaVail MM, Gorrin GM, Yasumura D, *et al.* Increased susceptibility to constant light in rr and pcd mice with inherited retinal degenerations. *Invest Ophthalmol Vis Sci* 1999;40:1020–4.
51 Reme CE, Weller M, Szczesny P, *et al.* Light-induced apoptosis in the rat retina in vivo. In: Anderson RE, LaVail MM, Hollyfield JG, eds. *Degenerative disease of the retina.* New York: Plenum, 1995:19–25.
52 Chen J, Flannery JG, LaVail MM, *et al.* bcl-2 overexpression reduces apoptotic photoreceptor cell death in three different retinal degenerations. *Proc Natl Acad Sci USA* 1996;93:7042–7.
53 Nir I, Kedzierski W, Chen J, *et al.* Expression of Bcl-2 protects against photoreceptor degeneration in retinal degeneration slow (rds) mice. *J Neurosci* 2000;20:2150–4.
54 Joseph RM, Li T. Overexpression of Bcl-2 or Bcl-XL transgenes and photoreceptor degeneration. *Invest Ophthalmol Vis Sci* 1996;37:2131–46.
55 Hanaoka K, Hayasaka M, Uetsuki T, *et al.* A stable cellular marker for the analysis of mouse chimeras: the bacterial chloramphenicol acetyltransferase gene driven by the human elongation factor 1 alpha promoter. *Differentiation* 1991;48:183–9.
56 Feinberg AP, Vogelstein B. A technique for radiolabeling DNA restriction endonuclease fragments to high specific activity. *Anal Biochem* 1983;132:6–13.
57 Ando T, Umezawa A, Suzuki A, *et al.* EAT/mcl-1, a member of the bcl-2 related genes, confers resistance to apoptosis induced by cis-diammine dichloroplatinum (II) via a p53-independent pathway. *Jpn J Cancer Res* 1998;89:1420–33.
58 Hanna N, Peri KG, Abran D, *et al.* Light induces peroxidation in retina by activating prostaglandin G/H synthase. *Free Radic Biol Med* 1997;23:885–97.
59 Chen E. Inhibition of cytochrome oxidase and blue-light damage in rat retina. *Graefes Arch Clin Exp Ophthalmol* 1993;231:416–23.
60 Williams TP and Howell WL. Action spectrum of retinal light-damage in albino rats. *Invest Ophthalmol Vis Sci* 1983; 24:285–7.
61 Hao W, Fong HK. Blue and ultraviolet light-absorbing opsin from the retinal pigment epithelium. *Biochemistry* 1996;35: 6251–6.
62 Wenzel A, Grimm C, Marti A, *et al.* c-fos controls the private pathway of light-induced apoptosis of retinal photoreceptors. *J Neurosci* 2000;20:81–8.
63 Reynolds JE, Yang T, Qian L, *et al.* Mcl-1, a member of the Bcl-2 family, delays apoptosis induced by c-Myc overexpression in Chinese hamster ovary cells. *Cancer Res* 1994;54:6318–52.
64 Zhou P, Qian L, Bieszczad CK, *et al.* Mcl-1 in transgenic mice promotes survival in a spectrum of hematopoietic cell types and immortalization in the myeloid lineage. *Blood* 1998;92:3226–39.
65 Sato T, Hanada M, Bodrug S, *et al.* Interactions among members of the Bcl-2 protein family analyzed with a yeast two-hybrid system. *Proc Natl Acad Sci USA* 1994;91:9238–42.
66 Sedlak TW, Oltvai ZN, Yang E, *et al.* Multiple Bcl-2 family members demonstrate selective dimerizations with Bax. *Proc Natl Acad Sci USA* 1995;92:7834–8.
67 Krajewski S, Bodrug S, Krajewska M, *et al.* Immunohistochemical analysis of Mcl-1 protein in human tissues. Differential regulation of Mcl-1 and Bcl-2 protein production suggests a unique role for Mcl-1 in control of programmed cell death in vivo. *Am J Pathol* 1995;146: 1309–19.
68 Tsang SH, Chen J, Kjeldbye H, *et al.* Retarding photoreceptor degeneration in Pdegrm1/Pdegrml mice by an apoptosis suppressor gene. *Invest Ophthalmol Vis Sci* 1997;38:943–50.
69 Oltvai ZN, Milliman CL, Korsmeyer SJ. Bcl-2 heterodimerizes in vivo with a conserved homolog, Bax, that accelerates programmed cell death. *Cell* 1993;74:609–19.
70 Yin XM, Oltvai ZN, Korsmeyer SJ. BH1 and BH2 domains of Bcl-2 are required for inhibition of apoptosis and heterodimerization with Bax. *Nature* 1994;369:321–3.
71 Cheng EH, Kirsch DG, Clem RJ, *et al.* Conversion of Bcl-2 to a Bax-like death effector by caspases. *Science* 1997;278: 1966–8.
72 Clem RJ, Cheng EH, Karp CL, *et al.* Modulation of cell death by Bcl-XL through caspase interaction. *Proc Natl Acad Sci USA* 1998;95:554–9.
73 McDonnell JM, Fushman D, Milliman CL, *et al.* Solution structure of the proapoptotic molecule BID: a structural basis for apoptotic agonists and antagonists. *Cell* 1999;96: 625–34.
74 Chou JJ, Li H, Salvesen GS, *et al.* Solution structure of BID, an intracellular amplifier of apoptotic signaling. *Cell* 1999; 96:615–24.
75 Gross A, McDonnell JM, Korsmeyer SJ. BCL-2 family members and the mitochondria in apoptosis. *Genes Dev* 1999;13:1899–911.
76 Akgul C, Moulding DA, White MR, *et al.* In vivo localisation and stability of human Mcl-1 using green fluorescent protein (GFP) fusion proteins. *FEBS Lett* 2000;478:72–6.

Leukemia (2001) 15, 1176–1184

www.nature.com/leu

A novel differentiation-inducing therapy for acute promyelocytic leukemia with a combination of arsenic trioxide and GM-CSF

A Muto[1], M Kizaki[1], C Kawamura[1], H Matsushita[1], Y Fukuchi[1], A Umezawa[2], T Yamada[2], J Hata[2], N Hozumi[3], K Yamato[4], M Ito[5], Y Ueyama[6] and Y Ikeda[1]

Departments of [1]Internal Medicine and [2]Pathology, Division of Hematology, Keio University School of Medicine, Tokyo; [3]Institute of Biological Science, Science University of Tokyo, Chiba; [4]Section of Molecular Cellular Oncology and Microbiology, Department of Oral Function Restitution, Division of Oral Health Sciences, Tokyo Medical and Dental University, Tokyo; [5]Central Institute for Experimental Animals, Kanagawa; and [6]Department of Pathology, Tokai University School of Medicine, Kanagawa, Japan

Arsenic trioxide (As_2O_3) effectively induces clinical remission via apoptosis in relapsed acute promyelocytic leukemia (APL). However, because this new anti-leukemic drug is also considered to be a poison, its possible adverse effects are a highly important issue related to its clinical use. We here investigated, both *in vitro* and *in vivo*, the effects of a combination of As_2O_3 and GM-CSF as a novel therapeutic approach for the treatment of APL. Treatment of both retinoic acid (RA)-sensitive and -resistant APL cell lines (NB4 and UF-1 cells, respectively), as well as primary APL cells with a combination of As_2O_3 and GM-CSF for 4 days resulted in inducing differentiation, but not apoptosis, to mature granulocytes. In addition, a combination of both agents induced degradation of the PML/RARα protein. GM-CSF was found to be associated with increased tyrosine phosphorylation of Jak2 kinase in both NB4 and UF-1 cells, and a specific inhibitor of Jak2, AG490, completely blocked the ability of GM-CSF to prevent apoptosis and induce differentiation of As_2O_3-treated UF-1 cells. In *in vivo* analysis, As_2O_3 induced differentiation of APL cells in a RA-resistant APL model of human GM-CSF-producing transgenic SCID mice that had a high level of human GM-CSF in their sera. In contrast, As_2O_3 alone diminished tumors in UF-1 cells transplanted into NOD/SCID mice via induction of apoptosis. In conclusion, a combination of As_2O_3 and GM-CSF appears to be a novel differentiation-inducing therapy in patients with APL, including relapsed or RA-resistant cases. *Leukemia* (2001) **15**, 1176–1184.
Keywords: acute promyelocytic leukemia (APL); arsenic trioxide; GM-CSF; apoptosis; differentiation

Introduction

Acute promyelocytic leukemia (APL) is characterized by a reciprocal chromosomal translocation, t(15;17), which generates a PML/RARα fusion protein between the PML gene on chromosome 15 and the RARα gene on chromosome 17.[1,2] The PML/RARα fusion protein blocks myeloid differentiation in a dominant negative manner and subsequently plays an important role in the leukemogenesis of APL.[3,4] Recent investigations have reported that all-*trans* retinoic acid (RA) induces a specific degradation of the PML/RARα fusion protein, possibly through a protease pathway, resulting in differentiation of APL cells into mature granulocytes.[5,6] Differentiation-inducing therapy is now the first choice treatment in patients with APL, and clinical studies have shown that nearly all patients who are treated with all-*trans* RA achieve complete remission.[7–10] However, such clinical remissions are usually brief, with APL cells quickly developing resistance to RA and relapse occurring in most patients.[11,12] Although most clinical approaches to overcoming RA resistance have been unsuccessful, recent reports from China and the US have shown that arsenic trioxide (As_2O_3) is an effective treatment for patients with APL, even for those refractory to all-*trans* RA.[13–15] As_2O_3 has been shown to induce apoptosis without differentiation of both the RA-sensitive NB4 cell line and its RA-resistant subclones, and this apoptosis may be mediated through down-regulation of Bcl-2 expression and modulation of the PML/RARα fusion protein.[16,17] More recently, it has been reported that As_2O_3 and the organic arsenical, melarsoprol, inhibit growth and induce apoptosis independent of both PML and PML/RARα expression in a variety of myeloid leukemic cell lines, suggesting that arsenic compounds may be useful for treatment of myeloid leukemias other than APL.[18] We have recently established a novel APL cell line (UF-1) with RA-resistant features.[19] Moreover, we have established a line of transgenic mice that produce human GM-CSF by means of a homozygous *scid* gene (hGMTgSCID), and have developed the first RA-resistant APL model in these mice.[20,21] Based on these model systems, we have reported that As_2O_3 can induce apoptosis of RA-resistant APL both *in vivo* and *in vitro*, and also induce differentiation *in vivo*.[22,23] However, the molecular mechanisms of As_2O_3-induced cellular differentiation of APL are still unclear. In addition, arsenicals are considered to be poisons and environmental carcinogens affecting the human skin, lung and other organs,[24] and they can induce serious side-effects including neurologic toxicity and cardiac and liver dysfunctions.[15] Cytokines such as GM-CSF, interleukin (IL)-3, and stem cell factor (SCF) regulate cell cycle progression, proliferation, and differentiation, as well as inhibit apoptosis of myeloid leukemic cells.[25,26] Therefore, a combination of As_2O_3 and cytokines might be a possible therapeutic approach for patients with newly diagnosed or relapsed APL.

We report in this study that a combination of As_2O_3 and GM-CSF induces differentiation, but not apoptosis, of APL cells *in vitro* and *in vivo* by modulating Jak2 tyrosine kinase. This combination therapy might be used as a novel differentiation-inducing therapy in patients with RA-resistant APL.

Materials and methods

Cell culture

The RA-resistant UF-1 APL cell line was established in our laboratory from a relapsed patient with APL who received all-*trans* RA.[19] Cells were maintained in RPMI 1640 medium (GIBCO-BRL, Gaitherburg, MD, USA) with 15% FCS (Hyclone Laboratories, Logan, MT, USA), 100 U/ml penicillin, and 100 mg/ml streptomycin in a humidified atmosphere with 5% CO_2. The RA-sensitive APL cell line, NB4, was kindly provided by Dr M Lanotte (Hôpital St Louis, Paris, France).[27] Fresh primary APL cells were obtained from bone marrow

Correspondence: M Kizaki, Division of Hematology, Keio University School of Medicine, 35 Shinanomachi, Shinjuku-ku, Tokyo 160–8582, Japan; Fax: +81-3-3353-3515
Received 27 October 2000; accepted 27 March 2001

after obtaining informed consent from two newly diagnosed patients with APL who presented with more than 80% blast cells. Confirmation of the presence of the PML/RARα gene was performed. Leukemic cells were isolated by the Lymphprep (Nycomed Pharma, Oslo, Norway) sedimentation procedure and resuspended in RPMI 1640 medium with 15% FCS. The morphology was evaluated from cytospine slide preparations with Giemsa staining, and the viability was assessed by trypan blue dye exclusion.

Chemicals and cytokines

As_2O_3 was purchased from Sigma Chemical (St Louis, MO, USA) and dissolved with PBS to a stock concentration of 10^{-4} M. Recombinant human granulocyte–macrophage colony-stimulating factor (GM-CSF) was kindly provided by Kirin Brewery Co., Ltd (Tokyo, Japan). Potent inhibitors of Jak2 tyrosine kinase (AG490), MAP kinase kinase (PD98059), and PI 3-kinase (Wortmannin) were purchased from Carbiochem (La Jolla, CA, USA). These agents were dissolved in DMSO (Sigma) and protected from light.

Assays for cellular proliferation

Cellular proliferation was measured by a viability and a non-radioactive cell proliferation assay system (MTT assay; Boehringer-Mannheim, Indianapolis, IN, USA). Cells were incubated with various concentrations of As_2O_3 (0–2 μM), GM-CSF (10 ng/ml) or a combination of both chemicals for 4 days in 96-well plates (Flow Laboratories, Irvine, CA, USA). Ten μl of MTT (5 μg/ml) was added to each well. The reaction was stopped after 4 h incubation by adding 100 μl of 0.04 N HCl in isopropanol, and the OD_{570} was determined. All experiments were performed at least three times, and the data were confirmed to be reproducible.

Analysis of apoptotic cells

Apoptotic cells were determined by morphological changes, as well as by staining with annexin V-FITC and propidium iodide (PI) labeling. Cells were stained with annexin V-FITC and PI double staining by using a staining kit purchased from PharMingen (San Diego, CA, USA), and these stained cells were analyzed using a FACScalibur flow cytometer (Becton Dickinson, San Jose, CA, USA).

Flow cytometric analysis

Induction of differentiation of APL cells into mature granulocytes or monocytes/macrophages was also assessed by changes and the expression of CD11b and CD14 antigens, respectively, by FACS analysis. Cells were incubated for 30 min with AB serum (Sigma) to block Fc receptors and were then stained using FITC-conjugated CD14 and PE-conjugated CD11b antibodies (Becton Dickinson). Control studies were performed with non-binding control mouse IgG_1 and IgG_{2a} isotype antibodies (Becton Dickinson). Cells were analyzed using a FACScalibur flow cytometer.

Western blotting and immunoblotting

For the detection of PML/RARα, cells were extracted by the method of Yoshida *et al*.[6] Briefly, cells were resuspended in buffer A (10 mM HEPES (pH 7.9), 1.5 mM $MgCl_2$, 10 mM KCl, 0.5 mM DTT, 0.42 M NaCl, 25% glycerol, 1.5 mg/ml protease inhibitors, 0.2 mM PMSF) for 10 min at 4°C. After centrifugation for 1 min at 600 *g*, cells were lysed in buffer A containing 0.2% NP40, 1.5 mg/ml protease inhibitors and 0.2 mM PMSF. The nuclei were pelleted and nuclear proteins were extracted in buffer B (20 mM HEPES (pH 7.9), 0.2 mM EDTA, 0.5 mM DTT, 0.42 M NaCl, 25% glycerol, 1.5 mg/ml protease inhibitors, 0.2 mM PMSF) for 20 min on ice. Cell lysates (10 μg of protein per lane) were fractionated in 12.5% SDS-polyacrylamide gels prior to transfer to the membrane (Immobilon-P membranes; Millipore, Bedford, MA, USA) by a standard protocol. Antibody binding was detected by using the enhanced chemiluminescence kit for Western blotting detection with hyper-ECL film (Amersham Japan, Tokyo, Japan). Blots were stained with Coomassie brilliant blue and were confirmed to contain a similar amount of protein extract in each lane. Antibodies used in this study were as follows: anti-RARα and -β-actin (Santa Cruz Biotechnology, Santa Cruz, CA, USA) and -PML (a gift from Dr T Naoe, Nagoya University, Nagoya, Japan). Also, rabbit anti-Jak1 and -Jak2 dual phosphospecific antibodies (Bio Science International, Camarillo, CA, USA) were used for the detection of phosphorylated Jak1 and Jak2. These antibodies did not cross-react with any other Jak or related proteins, and were specific for individual phosphorylated Jak proteins.

Animal model and experimental design

As previously described,[23] human GM-CSF-producing transgenic SCID (hGMTgSCID) mice were pretreated with 3 Gy of total body irradiation and then inoculated subcutaneously (s.c.) with UF-1 cells (1×10^7 cells) in their logarithmic growth phase. To assess the effects of As_2O_3 alone on tumor growth in SCID mice that do not overexpress hGM-CSF, UF-1 cells were also transplanted into NOD/SCID mice purchased from the Jackson Laboratory (Bar Harbor, ME, USA). All of these mice formed subcutaneous tumors at the injection site. Beginning at 40 days after implantation of the cells, 9.43 mg/kg body weight of As_2O_3 (LD_{50} of ICR mice) was injected s.c. into each separate tumor site daily for 21 days.[21] The tumor size was measured after treatment every week. When the mice showed severe wasting or when observations were finished, mice were sacrificed according to the UKCCCR guidelines, and the day of sacrifice was recorded.[28] Tumors were fixed in 4% paraformaldehyde, embedded in paraffin, sectioned, and then stained with hematoxylin and eosin for histological examination. For the immunohistochemical procedures, tumor sections were stained with rabbit anti-human LCA, MPO and neutrophil esterase polyclonal antibodies (DAKO Japan, Kyoto, Japan).

Results

Effects of As_2O_3 and GM-CSF in APL cell lines and primary APL cells in vitro

We examined the effects of a combination of As_2O_3 and GM-CSF on proliferation, differentiation and apoptosis of APL cell

lines and primary APL cells by means of morphology, MTT assay, and FACS analysis (Figure 1a–c). As previously reported,[16] exposure of both APL cell lines and primary cells to As_2O_3 alone resulted in the typical morphological appearance of apoptosis (Figure 1a, c). As_2O_3 inhibited the number of viable cells and the absorbance of MTT by both NB4 and UF-1 cells in a dose-dependent manner (Ref. 23 and Figure 2a). However, the combination of As_2O_3 and GM-CSF decreased the number of apoptotic cells (Figure 1b), suggesting that GM-CSF can protect against the induction of apoptosis in APL cells. Interestingly, the combination of As_2O_3 and GM-CSF induced differentiation of both RA-sensitive NB4 and RA-resistant UF-1 cells into mature granulocytes (Figures 1a and 2b). Based on the morphological study, GM-CSF control did not induce differentiation of primary APL cells (Figure 1c). In contrast, a combination of both agents also induced differentiation of primary APL cells from patients to mature granulocytes (Figure 1c). Both agents resulted in a 5.4-fold increase in expression of CD11b antigen in the primary APL cells as compared with controls (Figure 1c). As_2O_3 alone,

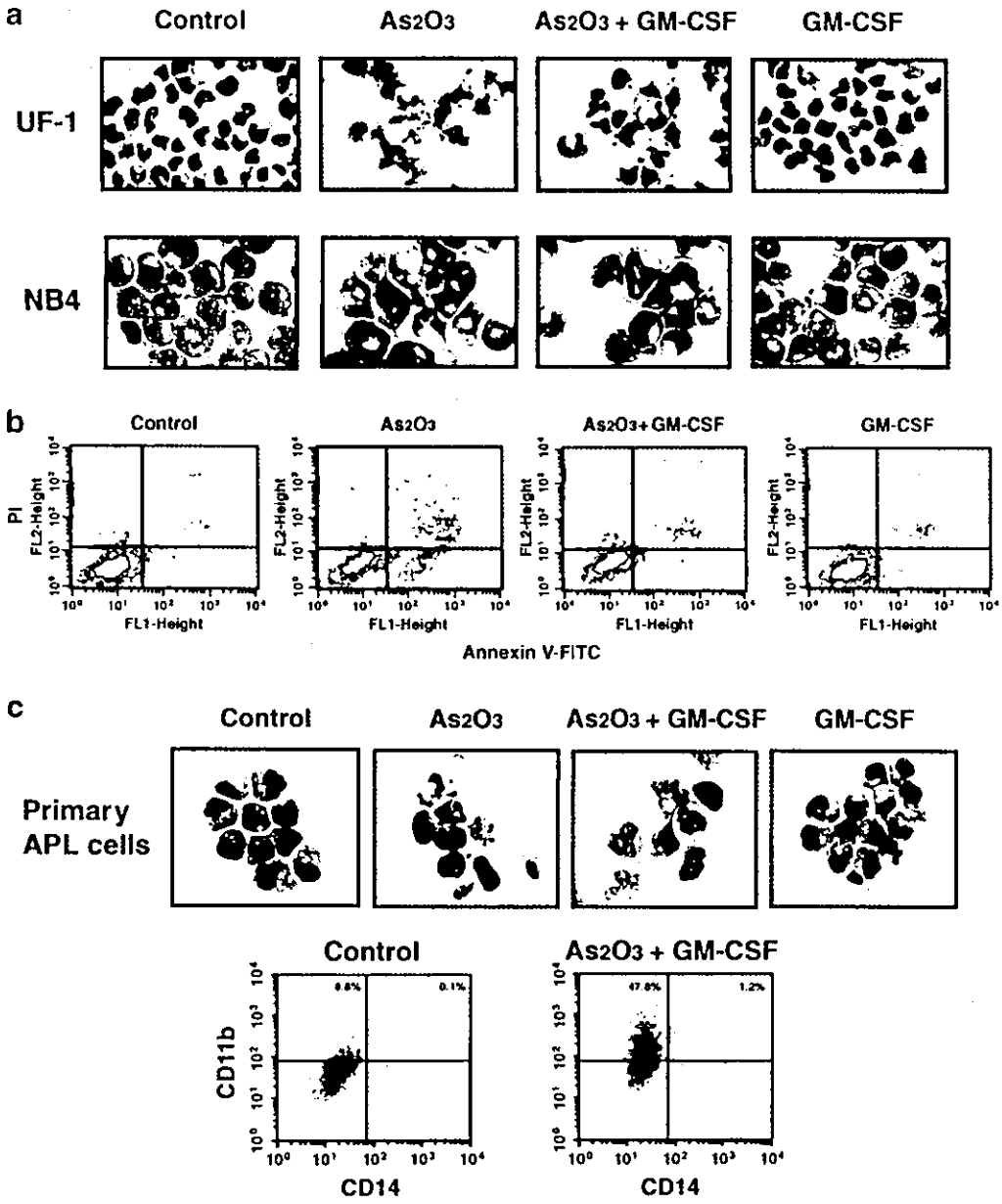

Figure 1 Effects of As_2O_3 and GM-CSF in APL cell lines and primary APL cells. (a) Morphological changes in RA-resistant UF-1 and RA-sensitive NB4 cells following treatment with GM-CSF, As_2O_3, or a combination of As_2O_3 and GM-CSF. Cells were cultured with GM-CSF (10 ng/ml), As_2O_3 (1 μM), or a combination of both agents for 4 days, and cytospine slides were prepared and stained with Giemsa. Original magnification ×1000. (b) Detection of apoptotic cells. UF-1 and NB4 cells were treated with GM-CSF, As_2O_3, or a combination of both chemicals, and prepared cells were stained with annexin V-FITC and PI. Representative data using UF-1 cells are shown. (c) Effects of GM-CSF, As_2O_3 or a combination of As_2O_3 and GM-CSF on primary APL cells. Morphological changes (upper panel) and the expression of CD11b and CD14 antigens by FACS analysis (lower panel) were examined. Controls in (a), (b) and (c) correspond to no treatment of the cells. For flow cytometric analysis, cells were incubated for 30 min with human AB serum to block Fc receptors and then stained with direct immunofluorescence using PE-conjugated mouse anti-human CD11b antibody. Control studies were performed with non-binding control mouse IgG1 and IgG2 isotype antibodies.

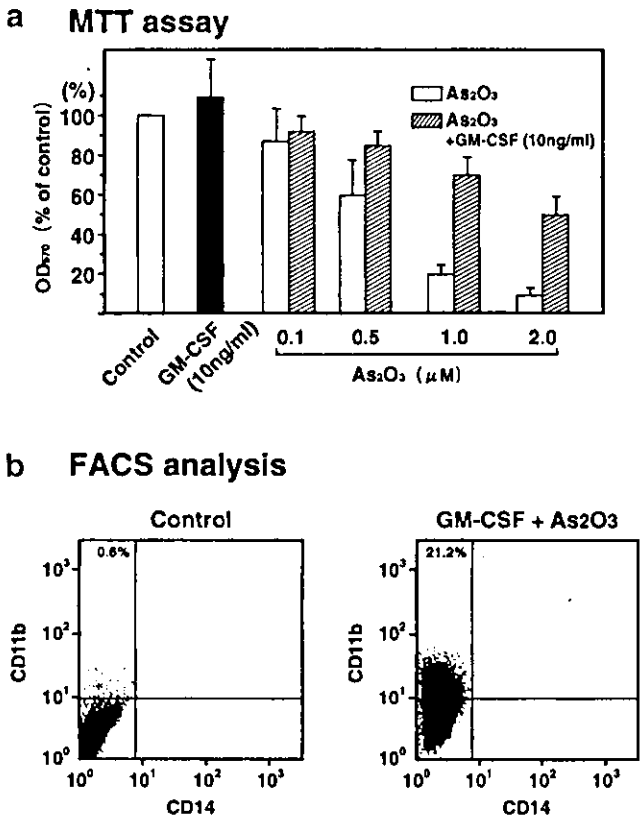

Figure 2 A combination of As_2O_3 and GM-CSF induced cellular differentiation of UF-1 cells. (a) MTT assay. UF-1 cells were cultured in 96-well plates with GM-CSF (10 ng/ml) alone or with the combination of GM-CSF (10 ng/ml) and various concentrations of As_2O_3 (0–2.0 μM) for 4 days, and then MTT incorporation was measured. The absorbance at 570 nm (OD_{570}) was recorded using an enzyme-linked immunosorbent plate reader. Results are presented as the means of triplicate experiments. Error bars represent the s.d. from experimental points in triplicate. (b) Expression of CD11b antigen by FACS analysis. UF-1 cells were treated with As_2O_3 alone (2.0 μM) or a combination of GM-CSF (10 ng/ml) and As_2O_3 for 4 days.

especially at a dosage of 1.0 or 2.0 μM, greatly suppressed the cellular proliferation of UF-1 cells; however, a combination of As_2O_3 and GM-CSF resulted in less inhibition (Figure 2a), suggesting that GM-CSF may prevent induction of apoptosis in UF-1 cells. In fact, a combination of GM-CSF (10 ng/ml) and As_2O_3 (2 μM) induced from 0.6% to 21.2% CD11b-positive UF-1 cells (Figure 2b). These results indicate that this combination of As_2O_3 and GM-CSF can induce differentiation, but not apoptosis, of APL cells *in vitro*.

Induction of PML/RARα chimeric protein degradation by a combination of As_2O_3 and GM-CSF

Previous studies have reported that all-*trans* RA and As_2O_3 individually induce a rapid degradation of PML/RARα, but not of the wild-type RARα protein.[6,13,17] NB4 and UF-1 cells were treated for 6 h with 1 μM As_2O_3, 10 ng/ml GM-CSF or As_2O_3 plus GM-CSF, and then subjected to Western blot analysis using anti-PML and anti-RARα antibodies (Figure 3a, b). In both RA-sensitive and -resistant APL cells, Western blot analysis using the anti-PML antibody showed that either As_2O_3 or a combination of As_2O_3 and GM-CSF could induce a total degradation of PML/RARα as well as the wild-type PML proteins, while GM-CSF alone did not degrade the chimeric protein (Figure 3a, b). Interestingly, GM-CSF alone increased expression of the PML protein in UF-1 cells, but not in NB4 cells. However, the reason for the discrepancy in the PML expression patterns between UF-1 and NB4 cells was unclear. We next performed Western blot analysis with the anti-RARα antibody. In this case, exposure to As_2O_3 with or without GM-CSF also led to degradation of expression of the PML/RARα protein, but did not change the levels of RARα (Figure 3a, b).

AG490, a specific inhibitor of Jak2 kinase, inhibits the As_2O_3 and GM-CSF-induced differentiation of APL cells

DNA synthesis and anti-apoptotic signals of GM-CSF are transduced via an interaction between the receptor β subunit and activated Jak2 tyrosine kinase.[29] The activation of Jak2 by GM-CSF leads to rapid tyrosine phosphorylation of the GM-CSF receptor β subunit and activates pathways that prevent cell death.[30] Thus, we examined the activation of Jak2 by As_2O_3, GM-CSF or a combination of both agents. As_2O_3 alone did not induce tyrosine phosphorylation of Jak2, but GM-CSF alone or a combination of As_2O_3 and GM-CSF did induce tyrosine phosphorylation of Jak2 in both NB4 and UF-1 cells (Figure 4a, b). Interestingly, activated Jak2 is decreased in both As_2O_3-treated NB4 and UF-1 cells (Figure 4a, b). In contrast, tyrosine phosphorylation of Jak1 was not induced by either As_2O_3, GM-CSF or a combination of both agents (Figure 4a, b). To examine the role of activation of the Jak2 kinase signaling pathways, we examined the effects of AG490, a specific inhibitor of Jak2 kinase, on As_2O_3 and GM-CSF-induced differentiation of APL cells. Exposure to a combination of As_2O_3 (1 μM) and GM-CSF (10 ng/ml) for 4 days resulted in differentiation of UF-1 cells into mature granulocytes by means of morphology and expression of CD11b antigen (Figure 5a, c). Although AG490 alone (5 μM) did not affect the proliferation and differentiation of UF-1 cells, AG490 in combination with As_2O_3 and GM-CSF reduced the number of CD11b-positive cells and induced apoptosis of UF-1 cells (Figure 5a–c). In contrast to the Jak2 kinase inhibitor, inhibitors of MAP kinase kinase (PD98059) and PI 3-kinase (Wortmannin) had no potent effects on the differentiation of APL cells induced by the combination of both chemicals (data not shown). Therefore, Jak2 kinase inhibitor specifically blocked the ability of GM-CSF to prevent apoptosis and induced differentiation of As_2O_3-treated APL cells.

Effects of As_2O_3 in vivo

We have previously established a human GM-CSF-producing transgenic SCID (hGMTgSCID) system in mice[20] and have developed the first human RA-resistant APL model in these SCID mice by using NB4 and UF-1 cells.[21] To address the direct effects of As_2O_3 on APL cells *in vivo*, we transplanted UF-1 cells into NOD/SCID mice to establish an *in vivo* APL model without endogenous hGM-CSF. Tumor size in NOD/SCID mice was decreased by treatment with As_2O_3 alone for 21 days (data not shown), which resulted in cells with a typical appearance of apoptosis in the tissue sections (Figure 6), suggesting that APL cells also responded to As_2O_3 alone *in vivo*. In contrast, hGMTgSCID mice have a high amount of GM-CSF in their sera (>1 ng/ml);[21] therefore, we examined here the combined effects of As_2O_3 and GM-CSF